Cell

Induction of Pluripotent Stem Cells from Mouse Embryonic and Adult Fibroblast Cultures by Defined Factors

Kazutoshi Takahashi[1] and Shinya Yamanaka[1,2,*]
[1]Department of Stem Cell Biology, Institute for Frontier Medical Sciences, Kyoto University, Kyoto 606-8507, Japan
[2]CREST, Japan Science and Technology Agency, Kawaguchi 332-0012, Japan
*Contact: yamanaka@frontier.kyoto-u.ac.jp
DOI 10.1016/j.cell.2006.07.024

SUMMARY

Differentiated cells can be reprogrammed to an embryonic-like state by transfer of nuclear contents into oocytes or by fusion with embryonic stem (ES) cells. Little is known about factors that induce this reprogramming. Here, we demonstrate induction of pluripotent stem cells from mouse embryonic or adult fibroblasts by introducing four factors, Oct3/4, Sox2, c-Myc, and Klf4, under ES cell culture conditions. Unexpectedly, Nanog was dispensable. These cells, which we designated iPS (induced pluripotent stem) cells, exhibit the morphology and growth properties of ES cells and express ES cell marker genes. Subcutaneous transplantation of iPS cells into nude mice resulted in tumors containing a variety of tissues from all three germ layers. Following injection into blastocysts, iPS cells contributed to mouse embryonic development. These data demonstrate that pluripotent stem cells can be directly generated from fibroblast cultures by the addition of only a few defined factors.

INTRODUCTION

Embryonic stem (ES) cells, which are derived from the inner cell mass of mammalian blastocysts, have the ability to grow indefinitely while maintaining pluripotency and the ability to differentiate into cells of all three germ layers (Evans and Kaufman, 1981; Martin, 1981). Human ES cells might be used to treat a host of diseases, such as Parkinson's disease, spinal cord injury, and diabetes (Thomson et al., 1998). However, there are ethical difficulties regarding the use of human embryos, as well as the problem of tissue rejection following transplantation in patients. One way to circumvent these issues is the generation of pluripotent cells directly from the patients' own cells.

Somatic cells can be reprogrammed by transferring their nuclear contents into oocytes (Wilmut et al., 1997) or by fusion with ES cells (Cowan et al., 2005; Tada et al., 2001), indicating that unfertilized eggs and ES cells contain factors that can confer totipotency or pluripotency to somatic cells. We hypothesized that the factors that play important roles in the maintenance of ES cell identity also play pivotal roles in the induction of pluripotency in somatic cells.

Several transcription factors, including Oct3/4 (Nichols et al., 1998; Niwa et al., 2000), Sox2 (Avilion et al., 2003), and Nanog (Chambers et al., 2003; Mitsui et al., 2003), function in the maintenance of pluripotency in both early embryos and ES cells. Several genes that are frequently upregulated in tumors, such as *Stat3* (Matsuda et al., 1999; Niwa et al., 1998), *E-Ras* (Takahashi et al., 2003), c-*myc* (Cartwright et al., 2005), *Klf4* (Li et al., 2005), and β-*catenin* (Kielman et al., 2002; Sato et al., 2004), have been shown to contribute to the long-term maintenance of the ES cell phenotype and the rapid proliferation of ES cells in culture. In addition, we have identified several other genes that are specifically expressed in ES cells (Maruyama et al., 2005; Mitsui et al., 2003).

In this study, we examined whether these factors could induce pluripotency in somatic cells. By combining four selected factors, we were able to generate pluripotent cells, which we call induced pluripotent stem (iPS) cells, directly from mouse embryonic or adult fibroblast cultures.

RESULTS

We selected 24 genes as candidates for factors that induce pluripotency in somatic cells, based on our hypothesis that such factors also play pivotal roles in the maintenance of ES cell identity (see Table S1 in the Supplemental Data available with this article online). For β-catenin, c-Myc, and Stat3, we used active forms, S33Y-β-catenin (Sadot et al., 2002), T58A-c-Myc (Chang et al., 2000), and Stat3-C (Bromberg et al., 1999), respectively. Because of the reported negative effect of Grb2 on pluripotency (Burdon et al., 1999; Cheng et al., 1998), we included its dominant-negative mutant Grb2ΔSH2 (Miyamoto et al., 2004) as 1 of the 24 candidates.

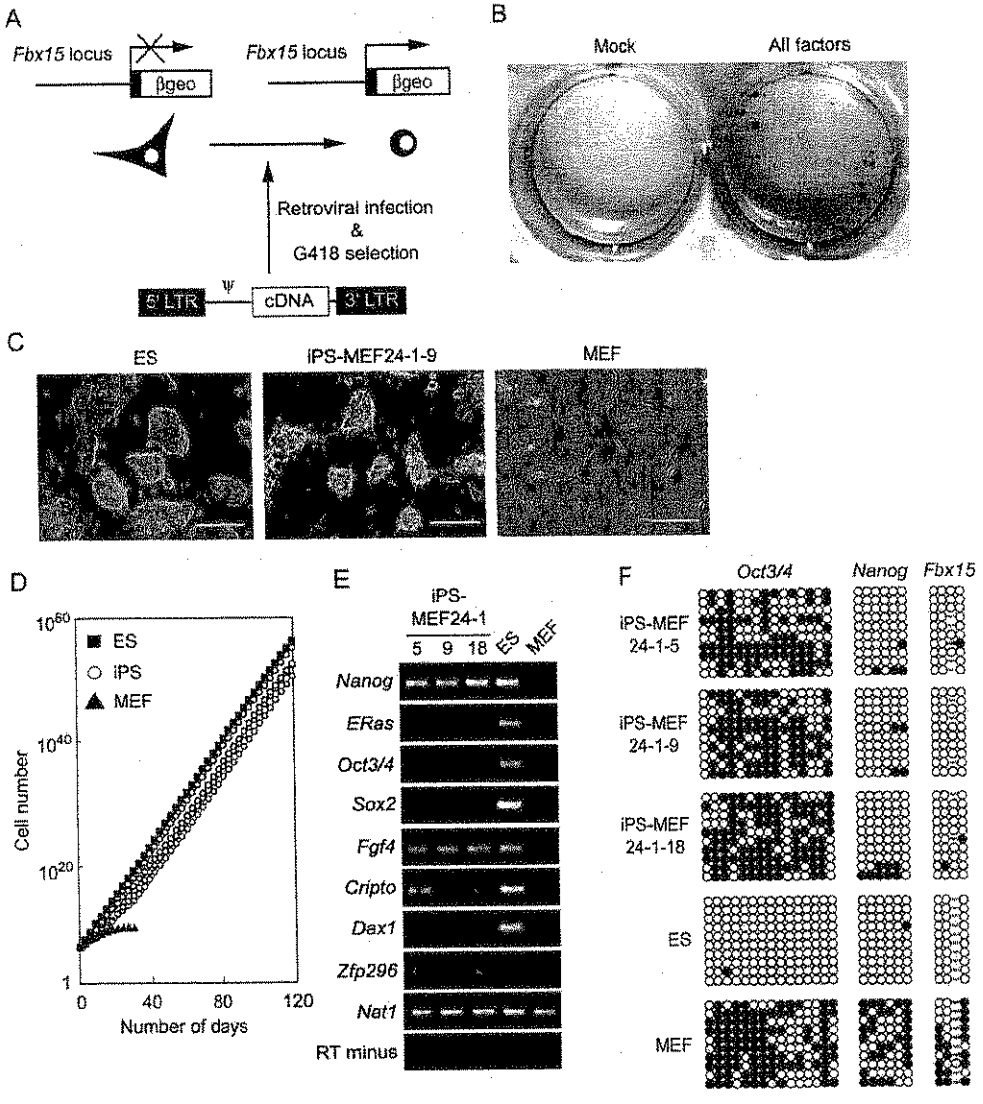

Figure 1. Generation of iPS Cells from MEF Cultures via 24 Factors

(A) Strategy to test candidate factors.

(B) G418-resistant colonies were observed 16 days after transduction with a combination of 24 factors. Cells were stained with crystal violet.

(C) Morphology of ES cells, iPS cells (iPS-MEF24, clone 1-9), and MEFs. Scale bars = 200 μm.

(D) Growth curves of ES cells, iPS cells (iPS-MEF24, clones 2-1–4), and MEFs. 3×10^5 cells were passaged every 3 days into each well of six-well plates.

(E) RT-PCR analysis of ES cell marker genes in iPS cells (iPS-MEF24, clones 1-5, 1-9, and 1-18), ES cells, and MEFs. *Nat1* was used as a loading control.

(F) Bisulfite genomic sequencing of the promoter regions of *Oct3/4*, *Nanog*, and *Fbx15* in iPS cells (iPS-MEF24, clones 1-5, 1-9, and 1-18), ES cells, and MEFs. Open circles indicate unmethylated CpG dinucleotides, while closed circles indicate methylated CpGs.

To evaluate these 24 candidate genes, we developed an assay system in which the induction of the pluripotent state could be detected as resistance to G418 (Figure 1A). We inserted a *βgeo* cassette (a fusion of the β-galactosidase and neomycin resistance genes) into the mouse *Fbx15* gene by homologous recombination (Tokuzawa et al., 2003). Although specifically expressed in mouse ES cells and early embryos, Fbx15 is dispensable for the maintenance of pluripotency and mouse development. ES cells homozygous for the βgeo knockin construct ($Fbx15^{\beta geo/\beta geo}$) were resistant to extremely high concentrations of G418 (up to 12 mg/ml), whereas somatic cells derived from $Fbx15^{\beta geo/\beta geo}$ mice were sensitive to a normal concentration of G418 (0.3 mg/ml). We expected that even partial activation of the *Fbx15* locus would result in resistance to normal concentrations of G418.

We introduced each of the 24 candidate genes into mouse embryonic fibroblasts (MEFs) from $Fbx15^{\beta geo/\beta geo}$

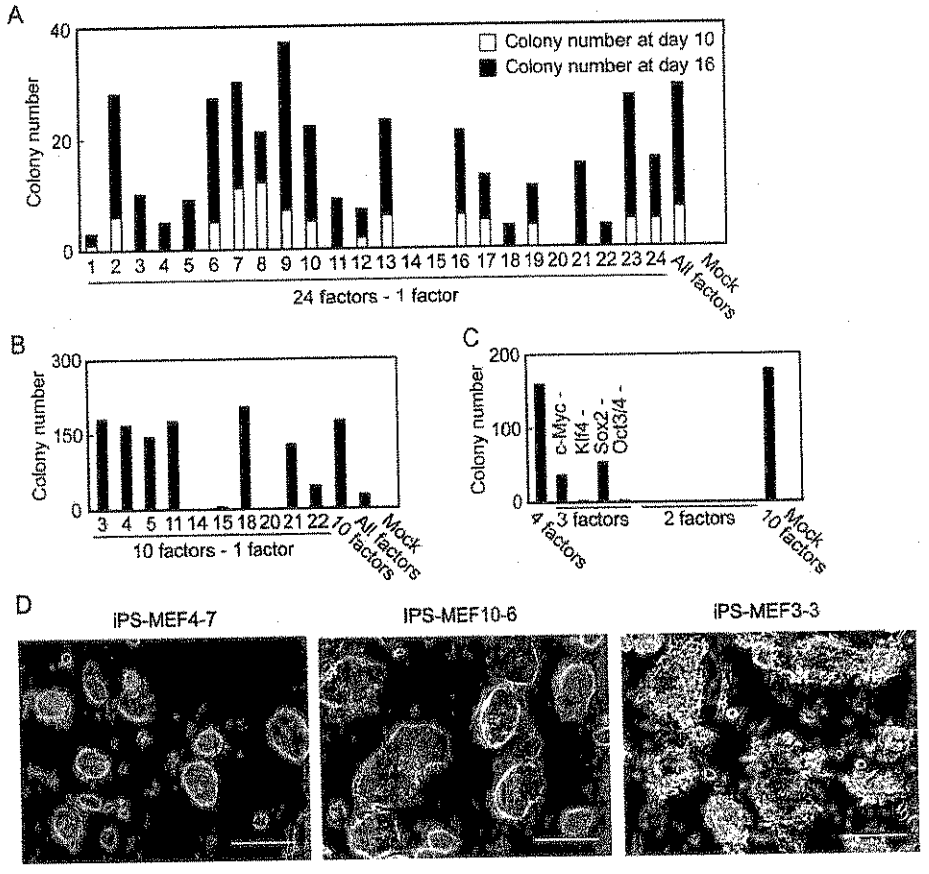

Figure 2. Narrowing down the Candidate Factors

(A) Effect of the removal of individual factors from the pool of 24 transduced factors on the formation of G418-resistant colonies. *Fbx15*$^{\beta geo/\beta geo}$ MEFs were transduced with the indicated factors and selected with G418 for 10 days (white columns) or 16 days (black columns).

(B) Effect of the removal of individual factors from the selected 10 factors on the formation of G418-resistant colonies 16 days after transduction.

(C) Effect of the transduction of pools of four, three, and two factors on the formation of G418-resistant colonies 16 days after transduction.

(D) Morphologies of iPS-MEF4 (clone 7), iPS-MEF10 (clone 6), and iPS-MEF3 (clone 3). Scale bars = 200 μm.

embryos by retroviral transduction (Morita et al., 2000). Transduced cells were then cultured on STO feeder cells in ES cell medium containing G418 (0.3 mg/ml). We did not, however, obtain drug-resistant colonies with any single factor, indicating that no single candidate gene was sufficient to activate the *Fbx15* locus (Figure 1B; see also Table S2, which summarizes all of the transduction experiments in this study).

In contrast, transduction of all 24 candidates together generated 22 G418-resistant colonies (Figure 1B). Of the 12 clones for which we continued cultivating under selection, 5 clones exhibited morphology similar to ES cells, including a round shape, large nucleoli, and scant cytoplasm (Figure 1C). We repeated the experiments and observed 29 G418-resistant colonies, from which we picked 6 colonies. Four of these clones possessed ES cell-like morphology and proliferation properties (Figure 1D). The doubling time of these cells (19.4, 17.5, 18.7, and 18.6 hr) was equivalent to that of ES cells (17.0 hr). We designated these cells iPS-MEF24 for "pluripotent stem cells induced from MEFs by 24 factors." Reverse transcription PCR (RT-PCR) analysis revealed that the iPS-MEF24 clones expressed ES cell markers, including *Oct3/4*, *Nanog*, *E-Ras*, *Cripto*, *Dax1*, and *Zfp296* (Mitsui et al., 2003) and *Fgf4* (Yuan et al., 1995) (Figure 1E). Bisulfite genomic sequencing demonstrated that the promoters of *Fbx15* and *Nanog* were demethylated in iPS cells (Figure 1F). By contrast, the *Oct3/4* promoter remained methylated in these cells. These data indicate that some combination of these 24 candidate factors induced the expression of ES cell marker genes in MEF culture.

Next, to determine which of the 24 candidates were critical, we examined the effect of withdrawal of individual factors from the pool of transduced candidate genes on the formation of G418-resistant colonies (Figure 2A). We identified 10 factors (3, 4, 5, 11, 14, 15, 18, 20, 21, and 22) whose individual withdrawal from the bulk transduction pool resulted in no colony formation 10 days after

transduction and fewer colonies 16 days after transduction. Combination of these 10 genes alone produced more ES cell-like colonies than transduction of all 24 genes did (Figure 2B).

We next examined the formation of colonies after withdrawal of individual factors from the 10-factor pool transduced into MEFs (Figure 2B). G418-resistant colonies did not form when either Oct3/4 (factor 14) or Klf4 (factor 20) was removed. Removal of Sox2 (factor 15) resulted in only a few G418-resistant colonies. When we removed c-Myc (factor 22), G418-resistant colonies did emerge, but these had a flatter, non-ES-cell-like morphology. Removal of the remaining factors did not significantly affect colony numbers. These results indicate that Oct3/4, Klf4, Sox2, and c-Myc play important roles in the generation of iPS cells from MEFs.

Combination of the four genes produced a number of G418-resistant colonies similar to that observed with the pool of 10 genes (Figure 2C). We continued cultivation of 12 clones for each transduction and were able to establish 4 iPS-MEF4 and 5 iPS-MEF10 clones. In addition, we could generate iPS cells (iPS-MEF4wt) with wild-type c-Myc instead of the T58A mutant (Table S2). These data demonstrate that iPS cells can be induced from MEF culture by the introduction of four transcription factors, Oct3/4, Sox2, c-Myc, and Klf4.

No combination of two factors could induce the formation of G418-resistant colonies (Figure 2C). Two combinations of three factors—Oct3/4, Sox2, and c-Myc (minus Klf4) or Klf4, Sox2, and c-Myc (minus Oct3/4)—generated a single, small colony in each case, but these could not be maintained in culture. With the combination of Oct3/4, Klf4, and Sox2 (minus c-Myc), we observed the formation of 36 G418-resistant colonies, which, however, exhibited a flat, non-ES-cell-like morphology. With the combination of Oct3/4, Klf4, and c-Myc (minus Sox2), we observed the formation of 54 G418-resistant colonies, of which we picked 6. Although all 6 clones could be maintained over several passages, the morphology of these cells (iPS-MEF3) differed from that of iPS-MEF4 and iPS-MEF10 cells, with iPS-MEF3 colonies exhibiting rough surfaces (Figure 2D). These data indicate that the combination of Oct3/4, c-Myc, and Klf4 can activate the *Fbx15* locus, but the change induced by these three factors alone is different from that seen in iPS-MEF4 or iPS-MEF10 cells.

We performed RT-PCR to examine whether ES cell marker genes were expressed in iPS cells (Figure 3A). We used primers that would amplify transcripts of the endogenous gene but not transcripts of the transgene. iPS-MEF10 and iPS-MEF4 clones expressed the majority of marker genes, with the exception of *Ecat1* (Mitsui et al., 2003). The expression of several marker genes, including *Oct3/4*, was higher in iPS-MEF4-7, iPS-MEF10-6, and iPS-MEF10-7 clones than in the remaining clones. *Sox2* was only expressed in iPS-MEF10-6. The iPS-MEF4wt clone also expressed many of the ES cell marker genes (Figure S1). Chromatin immunoprecipitation analyses showed that the promoters of *Oct3/4* and *Nanog* had increased acetylation of histone H3 and decreased dimethylation of lysine 9 of histone H3 (Figure 3B). CpG dinucleotides in these promoters remained partially methylated in iPS cells (Figure 3C). iPS-MEF4 and iPS-MEF10 cells were positive for alkaline phosphatase and SSEA-1 (Figure 3D) and showed high telomerase activity (Figure S2). These results demonstrate that iPS-MEF4 and iPS-MEF10 cells are similar, but not identical, to ES cells.

In iPS-MEF3 clones, *Ecat1*, *Esg1*, and *Sox2* were not activated (Figure 3A). *Nanog* was induced, but to a lesser extent than in iPS-MEF4 and iPS-MEF10 clones. *Oct3/4* was weakly activated in iPS-MEF3-3, -5, and -6 but was not activated in the remaining clones. By contrast, *E-Ras* and *Fgf4* were activated more efficiently in iPS-MEF3 than in iPS-MEF10 or iPS-MEF4. These data confirm that iPS-MEF3 cells are substantially different from iPS-MEF10 and iPS-MEF4 cells.

We compared the global gene-expression profiles of ES cells, iPS cells, and *Fbx15*$^{\beta geo/\beta geo}$ MEFs using DNA microarrays (Figure 4A). In addition, we examined *Fbx15*$^{\beta geo/\beta geo}$ MEFs in which the four factors had been introduced without G418 selection, immortalized MEFs expressing K-RasV12, and NIH 3T3 cells transformed with H-RasV12. Pearson correlation analysis revealed that iPS cells are clustered closely with ES cells but separately from fibroblasts and their derivatives (Figure 4A). The microarray analyses identified genes that were commonly upregulated in ES cells and iPS cells, including *Myb*, *Kit*, *Gdf3*, and *Zic3* (group I, Figure 4B and Table S3). Other genes were upregulated more efficiently in ES cells, iPS-MEF4, and iPS-MEF10 than in iPS-MEF3 clones, including *Dppa3*, *Dppa4*, *Dppa5*, *Nanog*, *Sox2*, *Esrrb*, and *Rex1* (group II). Lower expression of these genes may account for the lack of pluripotency in iPS-MEF3 cells. In addition, we found genes that were upregulated more prominently in ES cells than in iPS cells, including *Dnmt3a*, *Dnmt3b*, *Dnmt3l*, *Utf1*, *Tcl1*, and the *LIF receptor* gene (group III). These data confirm that iPS cells are similar, but not identical, to ES cells.

We examined the pluripotency of iPS cells by teratoma formation (Figure 5A; Table S6 and Figure S3). We obtained tumors with 5 iPS-MEF10 clones, 3 iPS-MEF4 clones, 1 iPS-MEF4wt clone, and 6 iPS-MEF3 clones after subcutaneous injection into nude mice. Histological examination revealed that 2 iPS-MEF10 clones (3 and 6), 2 iPS-MEF4 clones (2 and 7), and the iPS-MEF4wt-4 clone differentiated into all three germ layers, including neural tissues, cartilage, and columnar epithelium. iPS-MEF10-6 could give rise to all three germ layers even after 30 passages (Table S6 and Figure S3). We confirmed differentiation into neural and muscle tissues by immunostaining (Figure 5B) and RT-PCR (Figure S4). By contrast, these teratomas did not express the trophoblast marker *Cdx2* (Figure S4). iPS-MEF10-1 tumors differentiated into ectoderm and endoderm, but not mesoderm, and no signs of differentiation were observed in tumors derived from the remaining iPS-MEF10 (7 and 10) or from iPS-MEF4-10.

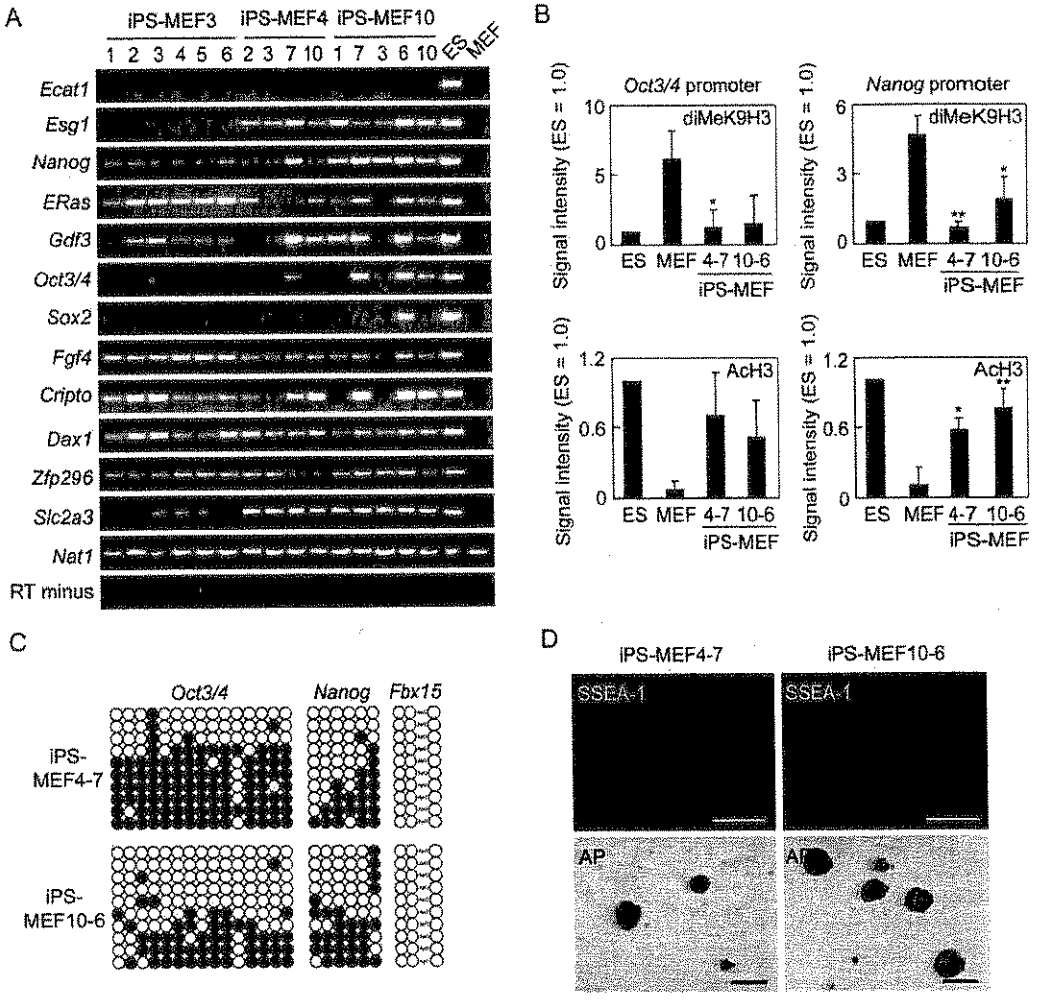

Figure 3. Gene-Expression Profiles of iPS Cells

(A) RT-PCR analysis of ES marker genes in iPS cells, ES cells, and MEFs. We used primer sets that amplified endogenous but not transgenic transcripts.

(B) The promoters of *Oct3/4* and *Nanog* were analyzed by ChIP for dimethylation status of lysine 9 of histone H3 and acetylation status of histone H3 in ES cells, MEFs, and iPS cells (MEF4-7 and MEF10-6). Data were quantified by real-time PCR. Shown are the averages and standard deviations of relative values compared to ES cells (n = 3). *$p < 0.05$; **$p < 0.01$ compared to MEFs.

(C) The promoters of *Oct3/4*, *Nanog*, and *Fbx15* were analyzed with bisulfite genomic sequencing for DNA methylation status in iPS-MEF4-7 and iPS-MEF10-6. The DNA methylation status of these promoters in ES cells and MEFs is shown in Figure 1F.

(D) iPS-MEF4-7 and iPS-MEF10-6 clones were stained with a mouse monoclonal antibody against SSEA-1 (480, Santa Cruz) or with an alkaline phosphatase kit (Sigma). Scale bars = 500 μm (SSEA1) and 1 mm (AP).

These data demonstrate that the majority of, but not all, iPS-MEF10 and iPS-MEF4 clones exhibit pluripotency.

In contrast, all tumors derived from iPS-MEF3 clones were composed entirely of undifferentiated cells (Table S6 and Figure S3). Thus, although the three factors (Oct3/4, c-Myc, and Klf4) could induce the expression of some ES cell marker genes, they were not able to induce pluripotency.

iPS-MEF10, iPS-MEF4, and iPS-MEF3 cells formed embryoid bodies in noncoated plastic dishes (Figure 5C). When grown in tissue culture dishes, the embryoid bodies from iPS-MEF10 and iPS-MEF4 cells attached to the dish bottom and initiated differentiation. After 3 days, immunostaining detected cells positive for α-smooth muscle actin (mesoderm marker), α-fetoprotein (endoderm marker), and βIII tubulin (ectoderm marker) (Figure 5D). By contrast, embryoid bodies from iPS-MEF3 cells remained undifferentiated even when cultured in gelatin-coated dishes (Figure 5C). These data confirmed pluripotency of iPS-MEF10 and iPS-MEF4 and nullipotency of iPS-MEF3 in vitro.

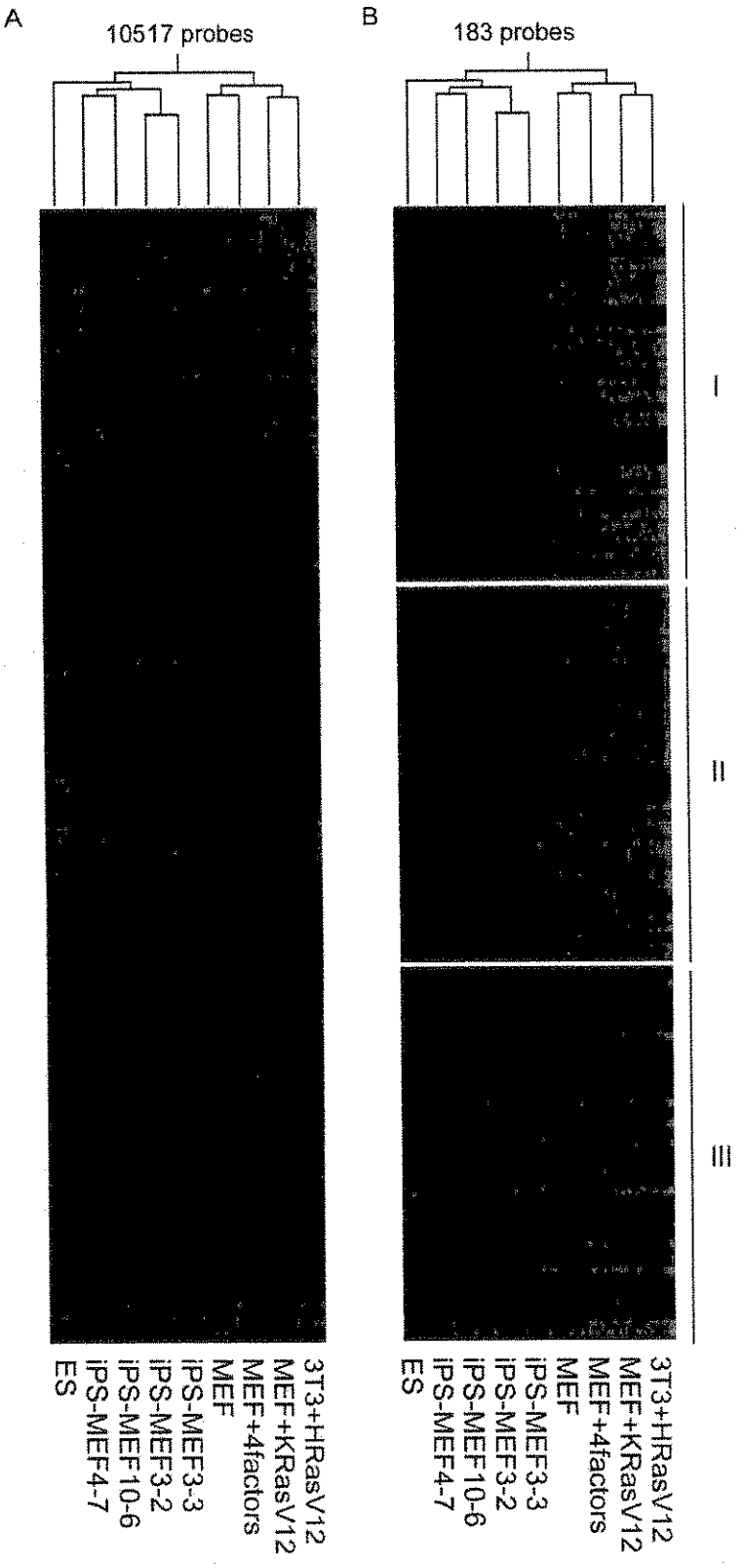

Figure 4. Global Gene-Expression Analyses by DNA Microarrays

(A) Pearson correlation analysis of 10,517 probes was performed to cluster ES cells, iPS cells (MEF4- 7, MEF10-6, MEF3-2, and MEF3-3), MEFs, MEFs expressing the four factors, immortalized MEFs expressing K-RasV12, and NIH 3T3 cells transformed by H-RasV12. Red indicates increased expression compared to median levels of the eight samples, whereas green means decreased expression.

(B) Genes upregulated in ES and/or iPS cells. Genes in group I are genes upregulated in ES cells and iPS cells. Genes in group II are upregulated more in ES cells, iPS-MEF4-7, and iPS-MEF10-6 than in iPS-MEF3 cells. Genes in group III are upregulated more in ES cells than in iPS cells. Lists of genes are shown in Tables S3–S5.

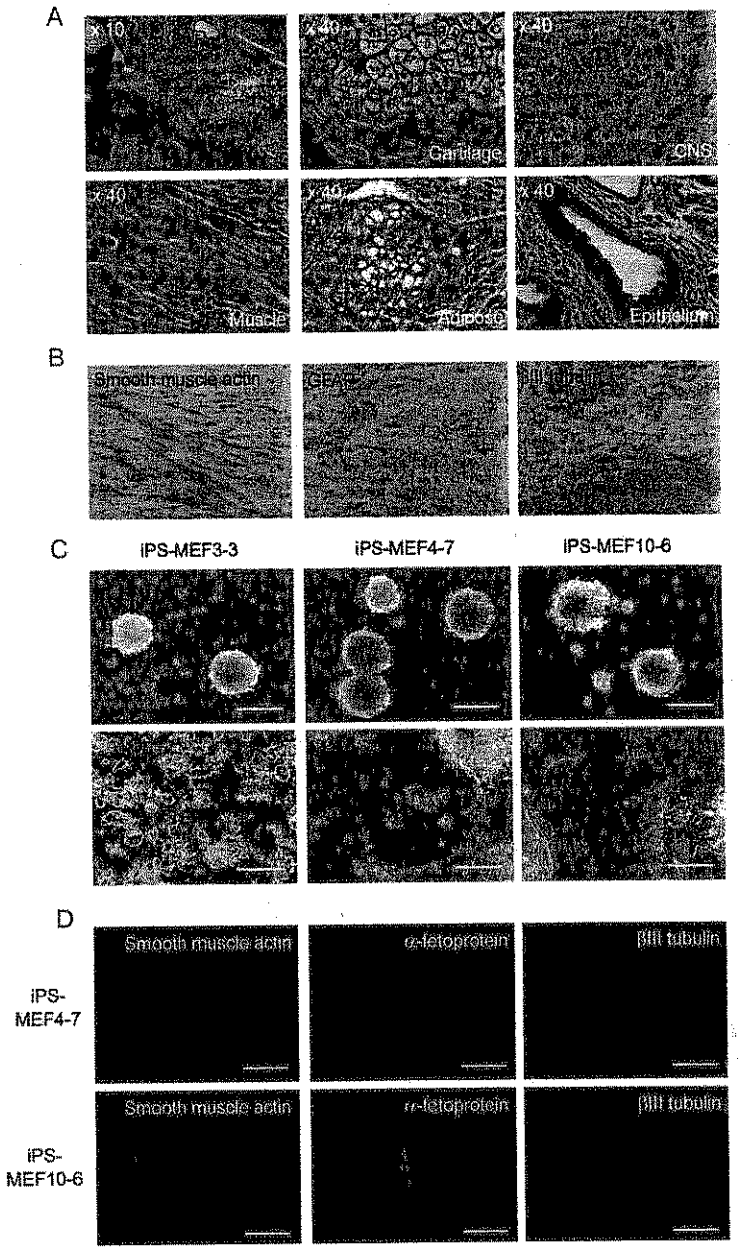

Figure 5. Pluripotency of iPS Cells Derived from MEFs

(A) Various tissues present in teratomas derived from iPS-MEF4-7 cells. Histology of other teratomas is shown in Figure S3 and Table S6.

(B) Immunostaining confirming differentiation into neural tissues and muscles in teratomas derived from iPS-MEF4-7.

(C) In vitro embryoid body formation (upper row) and differentiation (lower row). Scale bars = 200 μm.

(D) Immunostaining confirming in vitro differentiation into all three germ layers. Scale bars = 100 μm. Secondary antibodies were labeled with Cy3 (red), except for α-fetoprotein in iPS-MEF10-6, with which Alexa 488 (green) was used.

We next introduced the four selected factors into tail-tip fibroblasts (TTFs) of four 7-week-old male *Fbx15*$^{\beta geo/\beta geo}$ mice on a C57/BL6-129 hybrid background. We obtained 3 G418-resistant colonies, from each of which we could establish iPS cells (iPS-TTF4). We also introduced the four factors into TTFs from a 12-week-old female *Fbx15*$^{\beta geo/\beta geo}$ mouse, which also constitutively expressed green fluorescent protein (GFP) from the CAG promoter and had a C57/BL6-129-ICR hybrid background. Of the 13 G418-resistant colonies obtained, we isolated 6 clones from which we could establish iPS cells (iPS-TTFgfp4, clones 1–6). In addition, we established another iPS-TTFgfp4 (clone 7), in which the cDNA for each of the four factors was flanked with two loxP sites in the transgene. These cells were morphologically indistinguishable from ES cells (Figure 6A). RT-PCR showed that clones 3 and 7 of iPS-TTFgfp4 expressed the majority of ES cell marker genes at high levels and the others at lower levels (Figure 6B). In another attempt, we used either the T58A mutant or the wild-type c-Myc for transduction and established 5 iPS-TTFgfp4 clones (clones 8–12) and 3 iPS-TTFgfp4wt clones (clones 1–3) (Figure S5). RT-PCR

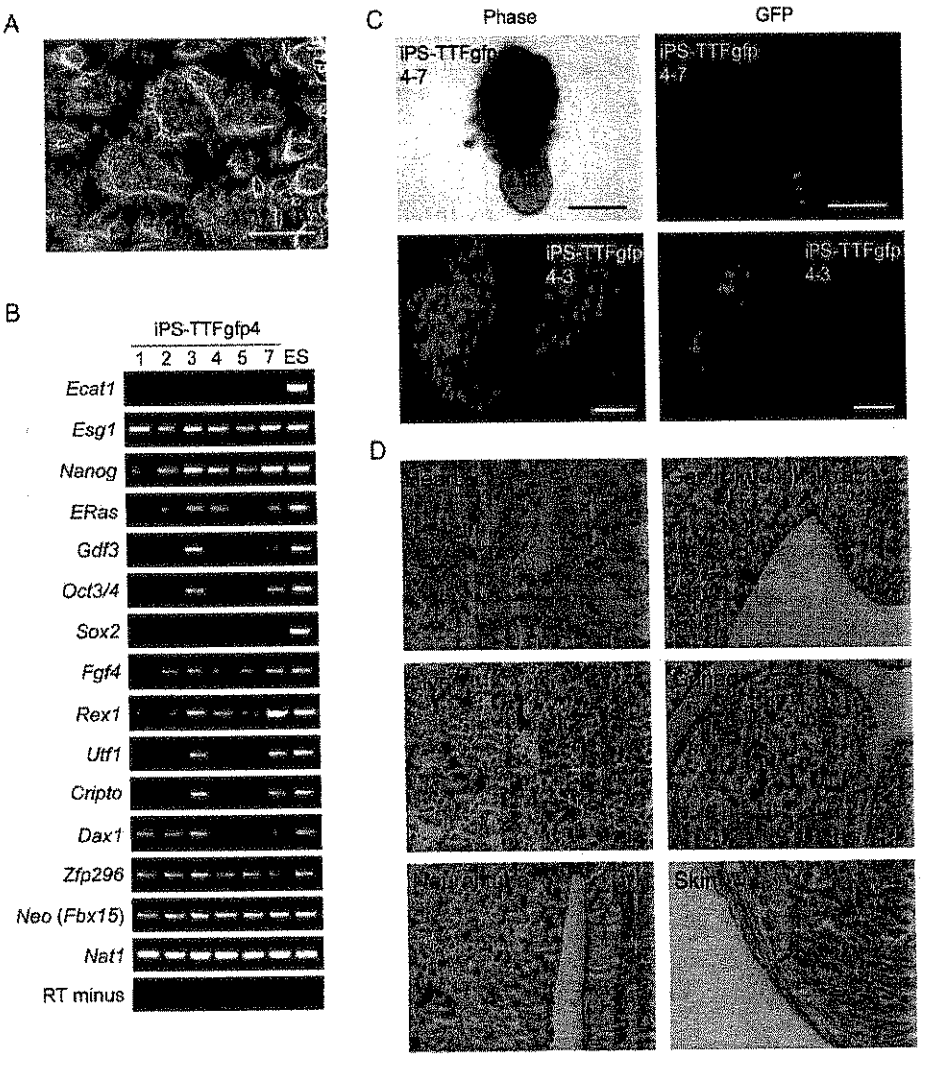

Figure 6. Characterization of iPS Cells Derived from Adult Mouse Tail-Tip Fibroblasts

(A) Morphology of iPS-TTFgfp4-3 on STO feeder cells.

(B) RT-PCR analysis of ES marker gene expression in iPS-TTFgfp4 cells (clones 1–5 and 7). We used primer sets that amplified endogenous but not transgenic transcripts.

(C) Contribution of iPS-TTFgfp4-7 and iPS-TTFgfp4-3 cells to mouse embryonic development. iPS cells were microinjected into C57/BL6 blastocysts. Embryos were analyzed with a fluorescence microscope at E7.5 (upper panels, iPS-TTFgfp4-7) or E13.5 (lower panels, iPS-TTFgfp4-3). Scale bars = 200 μm (upper panels) and 2 mm (lower panels).

(D) The E13.5 chimeric embryo was sectioned and stained with anti-GFP antibody (brown). Cells were counterstained with eosin (blue).

showed that iPS-TTFgfp4wt cells also expressed most of the ES cell marker genes (Figure S6).

We transplanted 2 iPS-TTF4 and 6 iPS-TTFgfp4 clones into nude mice, all of which produced tumors containing tissues of all three germ layers (Table S6 and Figure S3). We then introduced 2 clones of iPS-TTFgfp4 cells (clones 3 and 7) into C57/BL6 blastocysts by microinjection. With iPS-TTFgfp4-3, we obtained 18 embryos at E13.5, 2 of which showed contribution of GFP-positive iPS cells (Figure 6C). Histological analyses confirmed that iPS cells contributed to all three germ layers (Figure 6D). We observed GFP-positive cells in the gonad but could not determine whether they were germ cells or somatic cells. With iPS-TTFgfp4-7, we obtained 22 embryos at E7.5, 3 of which were positive for GFP. With the 2 clones, we had 27 pups born, but none of them were chimeric mice. In addition, iPS-TTFgfp4 cells could differentiate into all three germ layers in vitro (Figure S7). These data demonstrate that the four selected factors could induce pluripotent cells from adult mouse fibroblast cultures.

We further characterized the expression of the four factors and others in iPS cells. Real-time PCR confirmed that endogenous expression of *Oct3/4* and *Sox2* was lower in iPS cells than in ES cells (Figure S8). However, the total amount of the four factors from the endogenous genes and the transgenes exceeded the normal expression levels in ES cells. In contrast, Western blot analyses showed that the total protein amounts of the four factors in iPS cells were comparable to those in ES cells (Figure 7A; Figure S8). We could detect Nanog and E-Ras proteins in iPS cells, but at lower levels than those in ES cells (Figures 7A and 7B; Figure S8). The p53 levels in iPS cells were lower than those in MEFs and equivalent to those in ES cells (Figure 7A; Figure S9). The p21 levels in iPS cells varied in each clone and were between those in ES cells and MEFs (Figure S9). Upon differentiation in vitro, the total mRNA expression levels of *Oct3/4* and *Sox2* decreased but remained much higher than in ES cells. In contrast, their protein levels decreased to comparable levels in iPS cells and ES cells (Figure 7B).

Southern blot analyses showed that each iPS clone has a unique transgene integration pattern (Figure 7C). Karyotyping analyses of the iPS-TTFgfp4 (clones 1, 2, 3, 7, and 11) and iPS-TTFgfp4wt (clones 1–3) demonstrated that 2 iPS-TTFgfp4 clones and all of the iPS-TTFgfp4wt clones showed a normal karyotype of 40XX (Figure 7D), while the other 3 iPS-TTFgfp4 clones were 39XO, 40XO +10, and 40Xi(X). Analyses of PCR-based simple sequence length polymorphisms (SSLPs) demonstrated that iPS-MEF clones have a mixed background of C57/BL6 and 129 (Table S7), whereas iPS-TTFgfp clones have a mixed background of ICR, C57/BL6, and 129 (Table S8). Finally, we found that iPS cells could not remain undifferentiated when cultured in the absence of feeder cells, even with the presence of LIF (Figure 7E). These results, together with the different gene-expression patterns, exclude the possibility that iPS cells are merely contamination of preexisting ES cells. Finally, subclones of iPS cells were positive for alkaline phosphatase and could differentiate into all three germ layers in vitro (Figure S10), confirming their clonal nature.

DISCUSSION

Oct3/4, Sox2, and Nanog have been shown to function as core transcription factors in maintaining pluripotency (Boyer et al., 2005; Loh et al., 2006). Among the three, we found that Oct3/4 and Sox2 are essential for the generation of iPS cells. Surprisingly, Nanog is dispensable. In addition, we identified c-Myc and Klf4 as essential factors. These two tumor-related factors could not be replaced by other oncogenes including E-Ras, Tcl1, β-catenin, and Stat3 (Figures 2A and 2B).

The c-Myc protein has many downstream targets that enhance proliferation and transformation (Adhikary and Eilers, 2005), many of which may have roles in the generation of iPS cells. Of note, c-Myc associates with histone acetyltransferase (HAT) complexes, including TRRAP, which is a core subunit of the TIP60 and GCN5 HAT complexes (McMahon et al., 1998), CREB binding protein (CBP), and p300 (Vervoorts et al., 2003). Within the mammalian genome, there may be up to 25,000 c-Myc binding sites (Cawley et al., 2004), many more than the predicted number of Oct3/4 and Sox2 binding sites (Boyer et al., 2005; Loh et al., 2006). c-Myc protein may induce global histone acetylation (Fernandez et al., 2003), thus allowing Oct3/4 and Sox2 to bind to their specific target loci.

Klf4 has been shown to repress *p53* directly (Rowland et al., 2005), and p53 protein has been shown to suppress *Nanog* during ES cell differentiation (Lin et al., 2004). We found that iPS cells showed levels of p53 protein lower than those in MEFs (Figure 7A). Thus, Klf4 might contribute to activation of *Nanog* and other ES cell-specific genes through *p53* repression. Alternatively, Klf4 might function as an inhibitor of Myc-induced apoptosis through the repression of *p53* in our system (Zindy et al., 1998). On the other hand, Klf4 activates $p21^{CIP1}$, thereby suppressing cell proliferation (Zhang et al., 2000). This antiproliferation function of Klf4 might be inhibited by c-Myc, which suppresses the expression of $p21^{CIP1}$ (Seoane et al., 2002). The balance between c-Myc and Klf4 may be important for the generation of iPS cells.

One question that remains concerns the origin of our iPS cells. With our retroviral expression system, we estimated that only a small portion of cells expressing the four factors became iPS cells (Figure S11). The low frequency suggests that rare tissue stem/progenitor cells that coexisted in the fibroblast cultures might have given rise to the iPS cells. Indeed, multipotent stem cells have been isolated from skin (Dyce et al., 2004; Toma et al., 2001, 2005). These studies showed that ~0.067% of mouse skin cells are stem cells. One explanation for the low frequency of iPS cell derivation is that the four factors transform tissue stem cells. However, we found that the four factors induced iPS cells with comparably low efficiency even from bone marrow stroma, which should be more enriched in mesenchymal stem cells and other multipotent cells (Tables S2 and S6). Furthermore, cells induced by the three factors were nullipotent (Table S6 and Figure S3). DNA microarray analyses suggested that iPS-MEF4 cells and iPS-MEF3 cells have the same origin (Figure 4). These results do not favor multipotent tissue stem cells as the origin of iPS cells.

There are several other possibilities for the low frequency of iPS cell derivation. First, the levels of the four factors required for generation of pluripotent cells may have narrow ranges, and only a small portion of cells expressing all four of the factors at the right levels can acquire ES cell-like properties. Consistent with this idea, a mere 50% increase or decrease in Oct3/4 proteins induces differentiation of ES cells (Niwa et al., 2000). iPS clones overexpressed the four factors when RNA levels were analyzed, but their protein levels were comparable to those in ES cells (Figures 7A and 7B; Figure S8), suggesting that the iPS clones possess a mechanism (or mechanisms) that

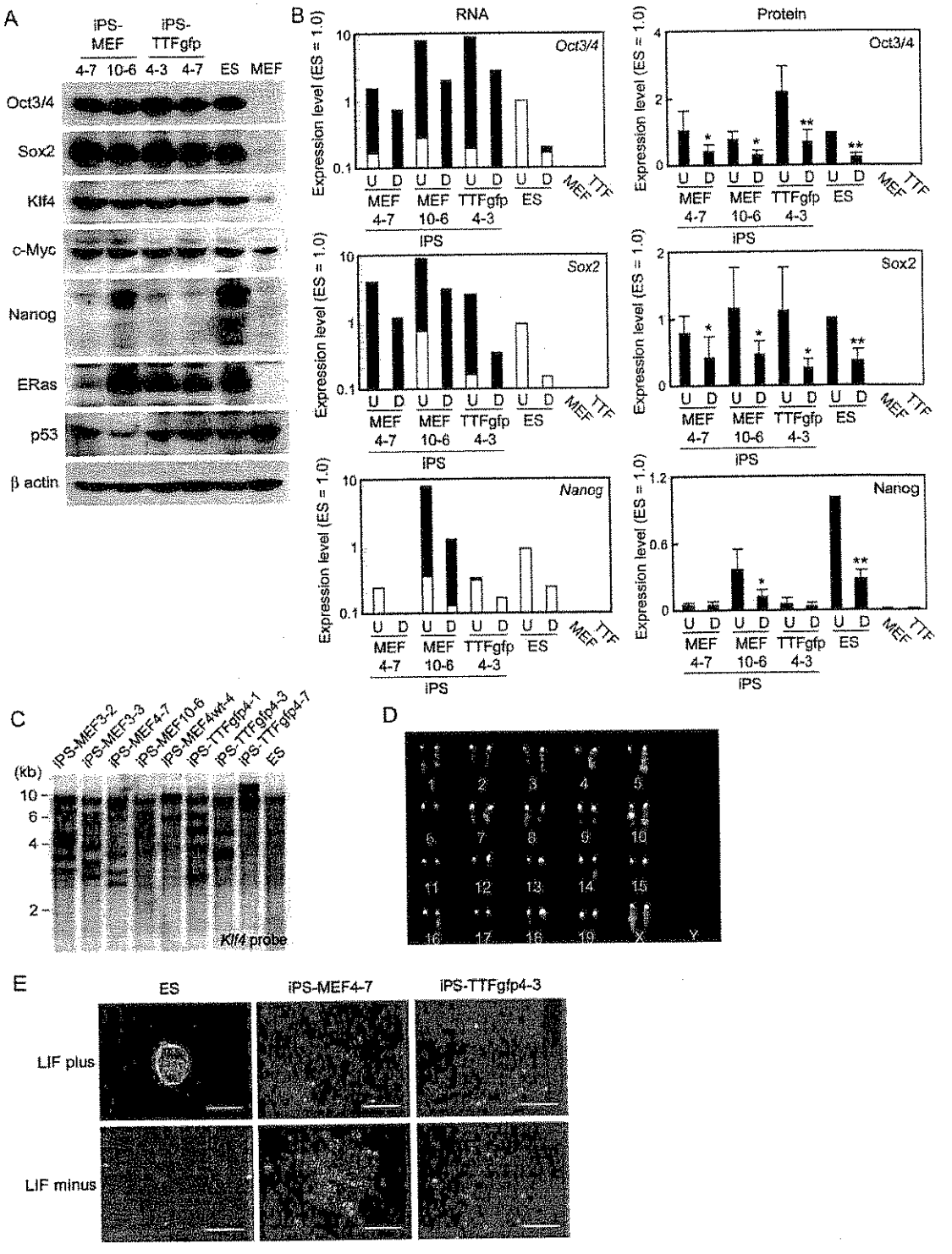

Figure 7. Biochemical and Genetic Analyses of iPS Cells

(A) Western blot analyses of the four factors and other proteins in iPS cells (MEF4-7, MEF10-6, TTFgfp4-3, and TTFgfp4-7), ES cells, and MEFs.

(B) Changes in RNA (left) and protein (right) levels of Oct3/4, Sox2, and Nanog in iPS cells and ES cells that were undifferentiated on STO feeder cells (U) or induced to differentiated in vitro through embryoid body formation (D). Shown are relative expression levels compared to undifferentiated ES cells. Data of MEFs and TTFs are also shown. RNA levels were determined with real-time PCR using primers specific for endogenous transcripts

tightly regulates the protein levels of the four factors. We speculate that high amounts of the four factors are required in the initial stage of iPS cell generation, but, once they acquire ES cell-like status, too much of the factors are detrimental for self-renewal. Only a small portion of transduced cells show such appropriate transgene expression. Second, generation of pluripotent cells may require additional chromosomal alterations, which take place spontaneously during culture or are induced by some of the four factors. Although the iPS-TTFgfp4 clones had largely normal karyotypes (Figure 7D), we cannot rule out the existence of minor chromosomal alterations. Site-specific retroviral insertion may also play a role. Southern blot analyses showed that each iPS clone has ~20 retroviral integrations (Figure 7C). Some of these may have caused silencing or fusion with endogenous genes. Further studies will be required to determine the origin of iPS cells.

Another unsolved question is whether the four factors we identified play roles in reprogramming induced by fusion with ES cells or nuclear transfer into oocytes. Since the four factors are expressed in ES cells at high levels, it is reasonable to speculate that they are involved in the reprogramming machinery that exists in ES cells. Our result is also consistent with the finding that the reprogramming activity resides in the nucleus, but not in the cytoplasm, of ES cells (Do and Scholer, 2004). However, iPS cells were not identical to ES cells, as shown by the global gene-expression patterns and DNA methylation status. It is possible that we have missed additional important factors. One such candidate is ECAT1, although its forced expression in iPS cells did not consistently upregulate ES cell marker genes (Figure S12).

More obscure are the roles of the four factors, especially Klf4 and c-Myc, in the reprogramming observed in oocytes. Both Klf4 and c-Myc are dispensable for preimplantation mouse development (Baudino et al., 2002; Katz et al., 2002). Furthermore, *c-myc* is not detected in oocytes (Domashenko et al., 1997). In contrast, *L-myc* is expressed maternally in oocytes. *Klf17* and *Klf7*, but not *Klf4*, are found in expressed sequence-tag libraries derived from unfertilized mouse eggs. Klf4 and c-Myc might be compensated by these related proteins. It is highly likely that other factors are also required to induce complete reprogramming and totipotency in oocytes.

It is likely that the four factors from the transgenes are required for maintaining the iPS cells since the expression of Oct3/4 and Sox2 from the endogenous genes remained low (Figure 7B; Figure S8). We intended to prove this by using transgenes flanked by two loxP sites and obtained an iPS clone (TTF4gfp4-7). However, we noticed that these cells contain multiple loxP sites on multiple chromosomes, and, thus, the Cre-mediated recombination would cause not only deletion of the transgenes but also inter- and intrachromosomal rearrangements. Studies with conditional expression systems, such as the tetracycline-mediated system, are required to answer this question.

We showed that the iPS cells can differentiate in vitro and in vivo even with the presence of the retroviral vectors containing the four factors. We found that Oct3/4 and Sox2 proteins decreased significantly during in vitro differentiation (Figure 7B). Retroviral expression has been shown to be suppressed in ES cells and further silenced upon differentiation by epigenetic modifications, such as DNA methylation (Yao et al., 2004). The same mechanisms are likely to play roles in transgene repression in iPS cells since they express *Dnmt3a*, *3b*, and *3l*, albeit at lower levels than ES cells do (Table S5). In addition, we found that iPS cells possess a mechanism (or mechanisms) that lowers protein levels of the transgenes and Nanog (Figure 7B; Figure S8). The same mechanism may be enhanced during differentiation. However, silencing of *Oct3/4* in iPS-TTFgfp4-3 cells was not complete, which may explain our inability to obtain live chimeric mice after blastocyst microinjection of iPS cells.

An unexpected finding in this study was the efficient activation of *Fgf4* and *Fbx15* by the combination of the three factors devoid of Sox2 since these two genes have been shown to be regulated synergistically by Oct3/4 and Sox2 (Tokuzawa et al., 2003; Yuan et al., 1995). It is also surprising that Nanog is dispensable for induction and maintenance of iPS cells. More detailed analyses of iPS cells will enhance our understanding of transcriptional regulation in pluripotent stem cells.

Our findings may have wider applications, as we have found that transgene reporters with other ES cell marker genes, such as *Nanog*, can replace the *Fbx15* knockin during selection (K. Okita and S.Y., unpublished data). However, we still do not know whether the four factors can generate pluripotent cells from human somatic cells. Use of c-Myc may not be suitable for clinical applications, and the process may require specific culture environments. Nevertheless, the finding is an important step in controlling pluripotency, which may eventually allow the creation of pluripotent cells directly from somatic cells of patients.

EXPERIMENTAL PROCEDURES

Mice

Fbx15$^{\beta geo/\beta geo}$ mice were generated with 129SvJae-derived RF8 ES cells as described previously (Tokuzawa et al., 2003) and were

(white columns) or those common for both endogenous and transgenic transcripts (white and black columns). RNA expression levels are shown on logarithmic axes. Protein levels were determined by Western blot normalized with β-actin. Protein levels are shown as the averages and standard deviations on linear axes (n = 4). *$p < 0.05$ compared to undifferentiated cells.

(C) Southern blot analyses showing the integration of transgenes. Genomic DNA isolated from iPS cells and ES cells was digested with EcoRI and BamHI, separated on agarose gel, transferred to a nylon membrane, and hybridized with a *Klf4* cDNA probe.

(D) Normal karyotype of iPS-TTFgfp4-2 clone.

(E) Morphology of ES cells and iPS cells cultured without feeder cells. One thousand cells were cultured on gelatin-coated six-well plates for 5 days, with or without LIF. Scale bars = 200 μm.

backcrossed to the C57/BL6 strain for at least five generations. These mice were used for primary mouse embryonic fibroblast (MEF) and tail-tip fibroblast (TTF) preparations. To generate *Fbx15*$^{\beta geo/\beta geo}$ mice with constitutive expression of GFP, an *Fbx15*$^{\beta geo/\beta geo}$ mouse (C57/BL6-129 background) was mated with an ICR mouse with the *GFP* transgene driven by the constitutive CAG promoter (Niwa et al., 1991). The resulting *Fbx15*$^{\beta geo/+,GFP/+}$ mice were intercrossed to generate *Fbx15*$^{\beta geo/\beta geo,GFP/GFP}$ mice. Nude mice (BALB/Jcl-nu) were purchased from CLEA.

Cell Culture

RF8 ES cells and iPS cells were maintained on feeder layers of mitomycin C-treated STO cells as previously described (Meiner et al., 1996). As a source of leukemia inhibitory factor (LIF), we used conditioned medium (1:10,000 dilution) from Plat-E cell cultures that had been transduced with a LIF-encoding vector. ES and iPS cells were passaged every 3 days. Plat-E packaging cells (Morita et al., 2000), which were also used to produce retroviruses, were maintained in DMEM containing 10% FBS, 50 units/50 μg/ml penicillin/streptomycin, 1 μg/ml puromycin (Sigma), and 100 μg/ml of blasticidin S (Funakoshi).

For MEF isolation, uteri isolated from 13.5-day-pregnant mice were washed with phosphate-buffered saline (PBS). The head and visceral tissues were removed from isolated embryos. The remaining bodies were washed in fresh PBS, minced using a pair of scissors, transferred into a 0.1 mM trypsin/1 mM EDTA solution (3 ml per embryo), and incubated at 37°C for 20 min. After incubation, an additional 3 ml per embryo of 0.1 mM trypsin/1 mM EDTA solution was added, and the mixture was incubated at 37°C for 20 min. After trypsinization, an equal amount of medium (6 ml per embryo DMEM containing 10% FBS) was added and pipetted up and down a few times to help with tissue dissociation. After incubation of the tissue/medium mixture for 5 min at room temperature, the supernatant was transferred into a new tube. Cells were collected by centrifugation (200 × g for 5 min at 4°C) and resuspended in fresh medium. 1 × 10^6 cells (passage 1) were cultured on 100 mm dishes at 37°C with 5% CO_2. In this study, we used MEFs within three passages to avoid replicative senescence.

To establish TTFs, the tails from adult mice were peeled, minced into 1 cm pieces, placed on culture dishes, and incubated in MF-start medium (Toyobo) for 5 days. Cells that migrated out of the graft pieces were transferred to new plates (passage 2) and maintained in DMEM containing 10% FBS. We used TTFs at passage 3 for iPS cell induction.

Retroviral Infection

The day before transduction, Plat-E cells (Morita et al., 2000) were seeded at 8 × 10^5 cells per 100 mm dish. On the next day, pMXs-based retroviral vectors were introduced into Plat-E cells using Fugene 6 transfection reagent (Roche) according to the manufacturer's recommendations. Twenty-seven microliters of Fugene 6 transfection reagent was diluted in 300 μl DMEM and incubated for 5 min at room temperature. Nine micrograms of plasmid DNA was added to the mixture, which was incubated for another 15 min at room temperature. After incubation, the DNA/Fugene 6 mixture was added drop by drop onto Plat-E cells. Cells were then incubated overnight at 37°C with 5% CO_2.

Twenty-four hours after transduction, the medium was replaced. MEFs or TTFs were seeded at 8 × 10^5 cells per 100 mm dish on mitomycin C-treated STO feeders. After 24 hr, virus-containing supernatants derived from these Plat-E cultures were filtered through a 0.45 μm cellulose acetate filter (Schleicher & Schuell) and supplemented with 4 μg/ml polybrene (Nacalai Tesque). Target cells were incubated in the virus/polybrene-containing supernatants for 4 hr to overnight. After infection, the cells were replated in 10 ml fresh medium. Three days after infection, we added G418 at a final concentration of 0.3 mg/ml. Clones were selected for 2 to 3 weeks.

Plasmid Construction

To generate pMXs-gw, we introduced a Gateway cassette rfA (invitrogen) into the EcoRI/XhoI site of the pMXs plasmid. Primers used are listed in Table S9. Mutations in β-*catenin*, *c-myc*, and *Stat3* were introduced by PCR-based site-directed mutagenesis. For forced expression, we amplified the coding regions of candidate genes by RT-PCR, cloned these sequences into pDONR201 or pENTR-D-TOPO (Invitrogen), and recombined the resulting plasmids with pMXs-gw by LR reaction (Invitrogen).

Teratoma Formation and Histological Analysis

ES cells or iPS cells were suspended at 1 × 10^7 cells/ml in DMEM containing 10% FBS. Nude mice were anesthetized with diethyl ether. We injected 100 μl of the cell suspension (1 × 10^6 cells) subcutaneously into the dorsal flank. Four weeks after the injection, tumors were surgically dissected from the mice. Samples were weighed, fixed in PBS containing 4% formaldehyde, and embedded in paraffin. Sections were stained with hematoxylin and eosin.

Bisulfite Genomic Sequencing

Bisulfite treatment was performed using the CpGenome modification kit (Chemicon) according to the manufacturer's recommendations. PCR primers are listed in Table S9. Amplified products were cloned into pCR2.1-TOPO (Invitrogen). Ten randomly selected clones were sequenced with the M13 forward and M13 reverse primers for each gene.

Determination of Karyotypes and SSLP by PCR

Karyotypes were determined with quinacrine-Hoechst staining at the International Council for Laboratory Animal Science (ICLAS) Monitoring Center (Japan). We obtained PCR primer sequences for SSLP from the Mouse Genome Informatics website (The Jackson Laboratory, http://www.informatics.jax.org). Allele sizes were approximated on the basis of the known allele sizes in various inbred strains.

Western Blot Analyses

Western blot was performed as previously described (Takahashi et al., 2003). The primary antibodies used were anti-Oct3/4 monoclonal antibody (C-10, Santa Cruz), anti-Sox2 antiserum (Maruyama et al., 2005), anti-Klf4 polyclonal antibody (H-180, Santa Cruz), anti-c-Myc polyclonal antibody (A-14, Santa Cruz), anti-Nanog antiserum (Mitsui et al., 2003), anti-E-Ras antiserum (Takahashi et al., 2003), anti-p53 polyclonal antibody (FL-393, Santa Cruz), and anti-β-actin monoclonal antibody (A5441, Sigma).

RT-PCR for Marker Genes

We performed reverse transcription reactions using ReverTra Ace -α- (Toyobo) and the oligo dT_{20} primer. PCR was done with ExTaq (Takara). Real-time PCR was performed with Platinum SYBR Green qPCR SuperMix-UDG with ROX (Invitrogen) according to manufacturer's instructions. Signals were detected with an ABI7300 Real-Time PCR System (Applied Biosystems). Primer sequences are listed in Table S9.

DNA Microarray

Total RNA from ES cells, iPS cells, or MEFs were labeled with Cy3. Samples were hybridized to a Mouse Oligo Microarray (G4121B, Agilent) according to the manufacturer's protocol. Arrays were scanned with a G2565BA Microarray Scanner System (Agilent). Data were analyzed using GeneSpring GX software (Agilent).

In Vitro Differentiation of iPS Cells

Cells were harvested by trypsinization and transferred to bacterial culture dishes in the ES medium without G418 or LIF. After 3 days, aggregated cells were plated onto gelatin-coated tissue culture dishes and incubated for another 3 days. The cells were stained with anti-α-smooth muscle actin monoclonal antibody (N1584, Dako), anti-α-fetoprotein polyclonal antibody (N1501, Dako) or anti-βIII tubulin monoclonal antibody (CBL412, Abcam) along with 4′-6-diamidino-2-phenylindole (Sigma). Total RNA derived from plated embryoid bodies on day 6 was used for RT-PCR analysis.

Chromatin Immunoprecipitation Assay

We performed chromatin immunoprecipitation (ChIP) as previously described (Maruyama et al., 2005). Antibodies used in this experiment were anti-dimethyl K9 H3 rabbit polyclonal antibody (ab7312-100, Abcam) and anti-acetyl H3 rabbit polyclonal antibody (06-599, Upstate). PCR primers are listed in Table S9.

Statistical Analyses

Data are shown as averages and standard deviations. We used Student's t test for protein-level analyses and one-factor ANOVA with Scheffe's post hoc test for ChIP analyses. All statistical analyses were done with Excel 2003 (Microsoft) with the Statcel2 add-on (OMS).

Supplemental Data

Supplemental Data include 12 figures and 9 tables and can be found with this article online at http://www.cell.com/cgi/content/full/126/4/■■■/DC1/.

ACKNOWLEDGMENTS

We are grateful to Tomoko Ichisaka for preparation of mice and Mitsuyo Maeda and Yoshinobu Toda for histological analyses. We thank Megumi Kumazaki, Mirei Murakami, Masayoshi Maruyama, and Noriko Tsubooka for technical assistance; Masato Nakagawa, Keisuke Okita, and Koji Shimozaki for scientific comments; and Yumi Ohuchi for administrative assistance. We also thank Dr. Robert Farese, Jr. for RF8 ES cells and Dr. Toshio Kitamura for the Plat-E cells and pMX retroviral vectors. This work was supported in part by research grants from the Ministry of Education, Culture, Sports, Science and Technology of Japan to S.Y. This work is also supported in part by the Takeda Science Foundation, the Osaka Cancer Research Foundation, the Inamori Foundation, the Mitsubishi Pharma Research Foundation, and the Sankyo Foundation of Life Science and by a Grant-in-Aid from the Japan Medical Association to S.Y. K.T. was supported by a fellowship from the Japan Society for the Promotion of Science.

Received: April 24, 2006
Revised: June 18, 2006
Accepted: July 20, 2006
Published online: August 10, 2006

REFERENCES

Adhikary, S., and Eilers, M. (2005). Transcriptional regulation and transformation by Myc proteins. Nat. Rev. Mol. Cell Biol. *6*, 635–645.

Avilion, A.A., Nicolis, S.K., Pevny, L.H., Perez, L., Vivian, N., and Lovell-Badge, R. (2003). Multipotent cell lineages in early mouse development depend on SOX2 function. Genes Dev. *17*, 126–140.

Baudino, T.A., McKay, C., Pendeville-Samain, H., Nilsson, J.A., Maclean, K.H., White, E.L., Davis, A.C., Ihle, J.N., and Cleveland, J.L. (2002). c-Myc is essential for vasculogenesis and angiogenesis during development and tumor progression. Genes Dev. *16*, 2530–2543.

Boyer, L.A., Lee, T.I., Cole, M.F., Johnstone, S.E., Levine, S.S., Zucker, J.P., Guenther, M.G., Kumar, R.M., Murray, H.L., Jenner, R.G., et al. (2005). Core transcriptional regulatory circuitry in human embryonic stem cells. Cell *122*, 947–956.

Bromberg, J.F., Wrzeszczynska, M.H., Devgan, G., Zhao, Y., Pestell, R.G., Albanese, C., and Darnell, J.E., Jr. (1999). Stat3 as an oncogene. Cell *98*, 295–303.

Burdon, T., Stracey, C., Chambers, I., Nichols, J., and Smith, A. (1999). Suppression of SHP-2 and ERK signalling promotes self-renewal of mouse embryonic stem cells. Dev. Biol. *210*, 30–43.

Cartwright, P., McLean, C., Sheppard, A., Rivett, D., Jones, K., and Dalton, S. (2005). LIF/STAT3 controls ES cell self-renewal and pluripotency by a Myc-dependent mechanism. Development *132*, 885–896.

Cawley, S., Bekiranov, S., Ng, H.H., Kapranov, P., Sekinger, E.A., Kampa, D., Piccolboni, A., Sementchenko, V., Cheng, J., Williams, A.J., et al. (2004). Unbiased mapping of transcription factor binding sites along human chromosomes 21 and 22 points to widespread regulation of noncoding RNAs. Cell *116*, 499–509.

Chambers, I., Colby, D., Robertson, M., Nichols, J., Lee, S., Tweedie, S., and Smith, A. (2003). Functional expression cloning of nanog, a pluripotency sustaining factor in embryonic stem cells. Cell *113*, 643–655.

Chang, D.W., Claassen, G.F., Hann, S.R., and Cole, M.D. (2000). The c-Myc transactivation domain is a direct modulator of apoptotic versus proliferative signals. Mol. Cell. Biol. *20*, 4309–4319.

Cheng, A.M., Saxton, T.M., Sakai, R., Kulkarni, S., Mbamalu, G., Vogel, W., Tortorice, C.G., Cardiff, R.D., Cross, J.C., Muller, W.J., and Pawson, T. (1998). Mammalian Grb2 regulates multiple steps in embryonic development and malignant transformation. Cell *95*, 793–803.

Cowan, C.A., Atienza, J., Melton, D.A., and Eggan, K. (2005). Nuclear reprogramming of somatic cells after fusion with human embryonic stem cells. Science *309*, 1369–1373.

Do, J.T., and Scholer, H.R. (2004). Nuclei of embryonic stem cells reprogram somatic cells. Stem Cells *22*, 941–949.

Domashenko, A.D., Latham, K.E., and Hatton, K.S. (1997). Expression of myc-family, myc-interacting, and myc-target genes during preimplantation mouse development. Mol. Reprod. Dev. *47*, 57–65.

Dyce, P.W., Zhu, H., Craig, J., and Li, J. (2004). Stem cells with multilineage potential derived from porcine skin. Biochem. Biophys. Res. Commun. *316*, 651–658.

Evans, M.J., and Kaufman, M.H. (1981). Establishment in culture of pluripotential cells from mouse embryos. Nature *292*, 154–156.

Fernandez, P.C., Frank, S.R., Wang, L., Schroeder, M., Liu, S., Greene, J., Cocito, A., and Amati, B. (2003). Genomic targets of the human c-Myc protein. Genes Dev. *17*, 1115–1129.

Katz, J.P., Perreault, N., Goldstein, B.G., Lee, C.S., Labosky, P.A., Yang, V.W., and Kaestner, K.H. (2002). The zinc-finger transcription factor Klf4 is required for terminal differentiation of goblet cells in the colon. Development *129*, 2619–2628.

Kielman, M.F., Rindapaa, M., Gaspar, C., van Poppel, N., Breukel, C., van Leeuwen, S., Taketo, M.M., Roberts, S., Smits, R., and Fodde, R. (2002). Apc modulates embryonic stem-cell differentiation by controlling the dosage of beta-catenin signaling. Nat. Genet. *32*, 594–605.

Li, Y., McClintick, J., Zhong, L., Edenberg, H.J., Yoder, M.C., and Chan, R.J. (2005). Murine embryonic stem cell differentiation is promoted by SOCS-3 and inhibited by the zinc finger transcription factor Klf4. Blood *105*, 635–637.

Lin, T., Chao, C., Saito, S., Mazur, S.J., Murphy, M.E., Appella, E., and Xu, Y. (2004). p53 induces differentiation of mouse embryonic stem cells by suppressing Nanog expression. Nat. Cell Biol. *7*, 165–171. Published online December 26, 2004. 10.1038/ncb1211.

Loh, Y.H., Wu, Q., Chew, J.L., Vega, V.B., Zhang, W., Chen, X., Bourque, G., George, J., Leong, B., Liu, J., et al. (2006). The Oct4 and Nanog transcription network regulates pluripotency in mouse embryonic stem cells. Nat. Genet. *38*, 431–440.

Martin, G.R. (1981). Isolation of a pluripotent cell line from early mouse embryos cultured in medium conditioned by teratocarcinoma stem cells. Proc. Natl. Acad. Sci. USA *78*, 7634–7638.

Maruyama, M., Ichisaka, T., Nakagawa, M., and Yamanaka, S. (2005). Differential roles for sox15 and sox2 in transcriptional control in mouse embryonic stem cells. J. Biol. Chem. *280*, 24371–24379.

Matsuda, T., Nakamura, T., Nakao, K., Arai, T., Katsuki, M., Heike, T., and Yokota, T. (1999). STAT3 activation is sufficient to maintain an

undifferentiated state of mouse embryonic stem cells. EMBO J. *18*, 4261–4269.

McMahon, S.B., Van Buskirk, H.A., Dugan, K.A., Copeland, T.D., and Cole, M.D. (1998). The novel ATM-related protein TRRAP is an essential cofactor for the c-Myc and E2F oncoproteins. Cell *94*, 363–374.

Meiner, V.L., Cases, S., Myers, H.M., Sande, E.R., Bellosta, S., Schambelan, M., Pitas, R.E., McGuire, J., Herz, J., and Farese, R.V., Jr. (1996). Disruption of the acyl-CoA:cholesterol acyltransferase gene in mice: evidence suggesting multiple cholesterol esterification enzymes in mammals. Proc. Natl. Acad. Sci. USA *93*, 14041–14046.

Mitsui, K., Tokuzawa, Y., Itoh, H., Segawa, K., Murakami, M., Takahashi, K., Maruyama, M., Maeda, M., and Yamanaka, S. (2003). The homeoprotein Nanog is required for maintenance of pluripotency in mouse epiblast and ES cells. Cell *113*, 631–642.

Miyamoto, Y., Yamauchi, J., Mizuno, N., and Itoh, H. (2004). The adaptor protein Nck1 mediates endothelin A receptor-regulated cell migration through the Cdc42-dependent c-Jun N-terminal kinase pathway. J. Biol. Chem. *279*, 34336–34342.

Morita, S., Kojima, T., and Kitamura, T. (2000). Plat-E: an efficient and stable system for transient packaging of retroviruses. Gene Ther. *7*, 1063–1066.

Nichols, J., Zevnik, B., Anastassiadis, K., Niwa, H., Klewe-Nebenius, D., Chambers, I., Scholer, H., and Smith, A. (1998). Formation of pluripotent stem cells in the mammalian embryo depends on the POU transcription factor Oct4. Cell *95*, 379–391.

Niwa, H., Yamamura, K., and Miyazaki, J. (1991). Efficient selection for high-expression transfectants with a novel eukaryotic vector. Gene *108*, 193–199.

Niwa, H., Burdon, T., Chambers, I., and Smith, A. (1998). Self-renewal of pluripotent embryonic stem cells is mediated via activation of STAT3. Genes Dev. *12*, 2048–2060.

Niwa, H., Miyazaki, J., and Smith, A.G. (2000). Quantitative expression of Oct-3/4 defines differentiation, dedifferentiation or self-renewal of ES cells. Nat. Genet. *24*, 372–376.

Rowland, B.D., Bernards, R., and Peeper, D.S. (2005). The KLF4 tumour suppressor is a transcriptional repressor of p53 that acts as a context-dependent oncogene. Nat. Cell Biol. *7*, 1074–1082.

Sadot, E., Conacci-Sorrell, M., Zhurinsky, J., Shnizer, D., Lando, Z., Zharhary, D., Kam, Z., Ben-Ze'ev, A., and Geiger, B. (2002). Regulation of S33/S37 phosphorylated beta-catenin in normal and transformed cells. J. Cell Sci. *115*, 2771–2780.

Sato, N., Meijer, L., Skaltsounis, L., Greengard, P., and Brivanlou, A.H. (2004). Maintenance of pluripotency in human and mouse embryonic stem cells through activation of Wnt signaling by a pharmacological GSK-3-specific inhibitor. Nat. Med. *10*, 55–63.

Seoane, J., Le, H.V., and Massague, J. (2002). Myc suppression of the p21(Cip1) Cdk inhibitor influences the outcome of the p53 response to DNA damage. Nature *419*, 729–734.

Tada, M., Takahama, Y., Abe, K., Nakatsuji, N., and Tada, T. (2001). Nuclear reprogramming of somatic cells by in vitro hybridization with ES cells. Curr. Biol. *11*, 1553–1558.

Takahashi, K., Mitsui, K., and Yamanaka, S. (2003). Role of ERas in promoting tumour-like properties in mouse embryonic stem cells. Nature *423*, 541–545.

Thomson, J.A., Itskovitz-Eldor, J., Shapiro, S.S., Waknitz, M.A., Swiergiel, J.J., Marshall, V.S., and Jones, J.M. (1998). Embryonic stem cell lines derived from human blastocysts. Science *282*, 1145–1147.

Tokuzawa, Y., Kaiho, E., Maruyama, M., Takahashi, K., Mitsui, K., Maeda, M., Niwa, H., and Yamanaka, S. (2003). Fbx15 is a novel target of Oct3/4 but is dispensable for embryonic stem cell self-renewal and mouse development. Mol. Cell. Biol. *23*, 2699–2708.

Toma, J.G., Akhavan, M., Fernandes, K.J., Barnabe-Heider, F., Sadikot, A., Kaplan, D.R., and Miller, F.D. (2001). Isolation of multipotent adult stem cells from the dermis of mammalian skin. Nat. Cell Biol. *3*, 778–784.

Toma, J.G., McKenzie, I.A., Bagli, D., and Miller, F.D. (2005). Isolation and characterization of multipotent skin-derived precursors from human skin. Stem Cells *23*, 727–737.

Vervoorts, J., Luscher-Firzlaff, J.M., Rottmann, S., Lilischkis, R., Walsemann, G., Dohmann, K., Austen, M., and Luscher, B. (2003). Stimulation of c-MYC transcriptional activity and acetylation by recruitment of the cofactor CBP. EMBO Rep. *4*, 484–490.

Wilmut, I., Schnieke, A.E., McWhir, J., Kind, A.J., and Campbell, K.H. (1997). Viable offspring derived from fetal and adult mammalian cells. Nature *385*, 810–813.

Yao, S., Sukonnik, T., Kean, T., Bharadwaj, R.R., Pasceri, P., and Ellis, J. (2004). Retrovirus silencing, variegation, extinction, and memory are controlled by a dynamic interplay of multiple epigenetic modifications. Mol. Ther. *10*, 27–36.

Yuan, H., Corbi, N., Basilico, C., and Dailey, L. (1995). Developmental-specific activity of the FGF-4 enhancer requires the synergistic action of Sox2 and Oct-3. Genes Dev. *9*, 2635–2645.

Zhang, W., Geiman, D.E., Shields, J.M., Dang, D.T., Mahatan, C.S., Kaestner, K.H., Biggs, J.R., Kraft, A.S., and Yang, V.W. (2000). The gut-enriched Kruppel-like factor (Kruppel-like factor 4) mediates the transactivating effect of p53 on the p21WAF1/Cip1 promoter. J. Biol. Chem. *275*, 18391–18398.

Zindy, F., Eischen, C.M., Randle, D.H., Kamijo, T., Cleveland, J.L., Sherr, C.J., and Roussel, M.F. (1998). Myc signaling via the ARF tumor suppressor regulates p53-dependent apoptosis and immortalization. Genes Dev. *12*, 2424–2433.

Accession Numbers

Microarray data are available in GEO (Gene Expression Omnibus, http://www.ncbi.nlm.nih.gov/projects/geo/index.cgi) with the accession number GSE5259.

Cell, Volume *126*

Supplemental Data

Induction of Pluripotent Stem Cells from Mouse Embryonic and Adult Fibroblast Cultures by Defined Factors

Kazutoshi Takahashi and Shinya Yamanaka

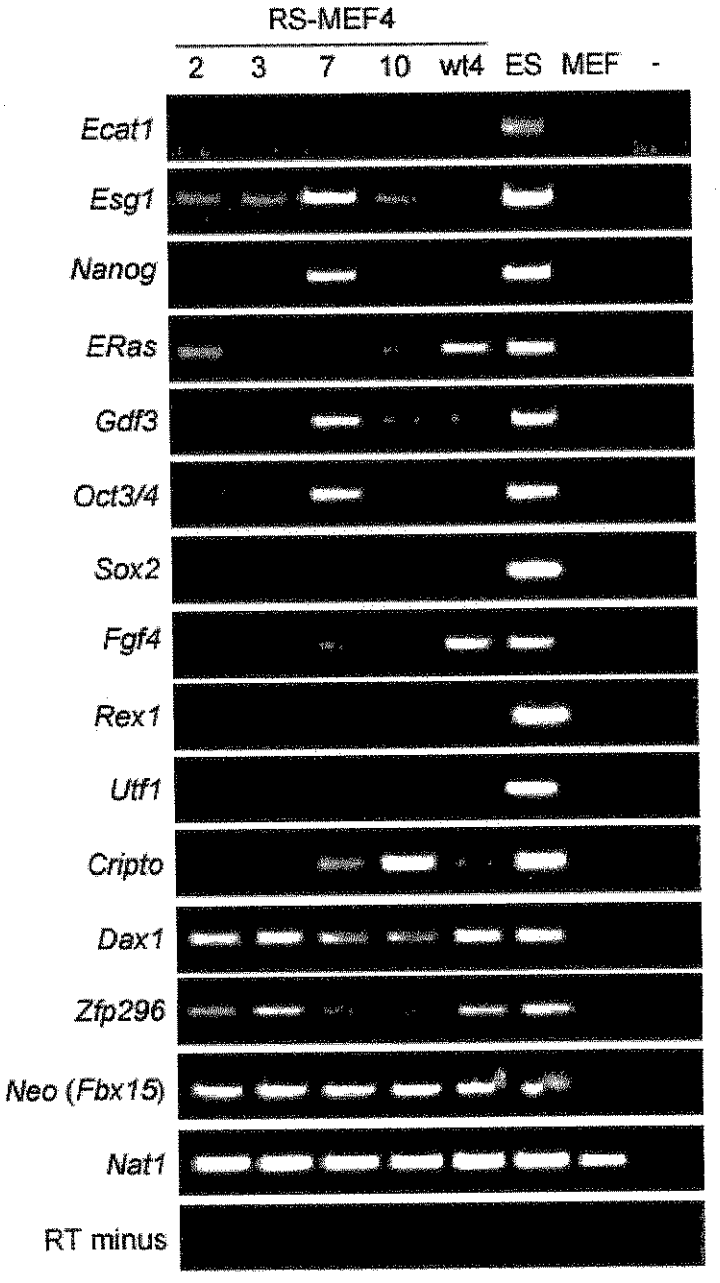

Figure S1. The Expression Patterns of ES Cell Marker Genes in the iPS Clones Established by Wild-Type c-Myc or the T58A Mutant

We performed RT-PCR with total RNA isolated from iPS clones (iPS-MEF4-2, 4-3, 4-7, 4-10 and 4wt-4), ES cells, and MEFs. We used primers that only amplified the endogenous genes (Table S9).

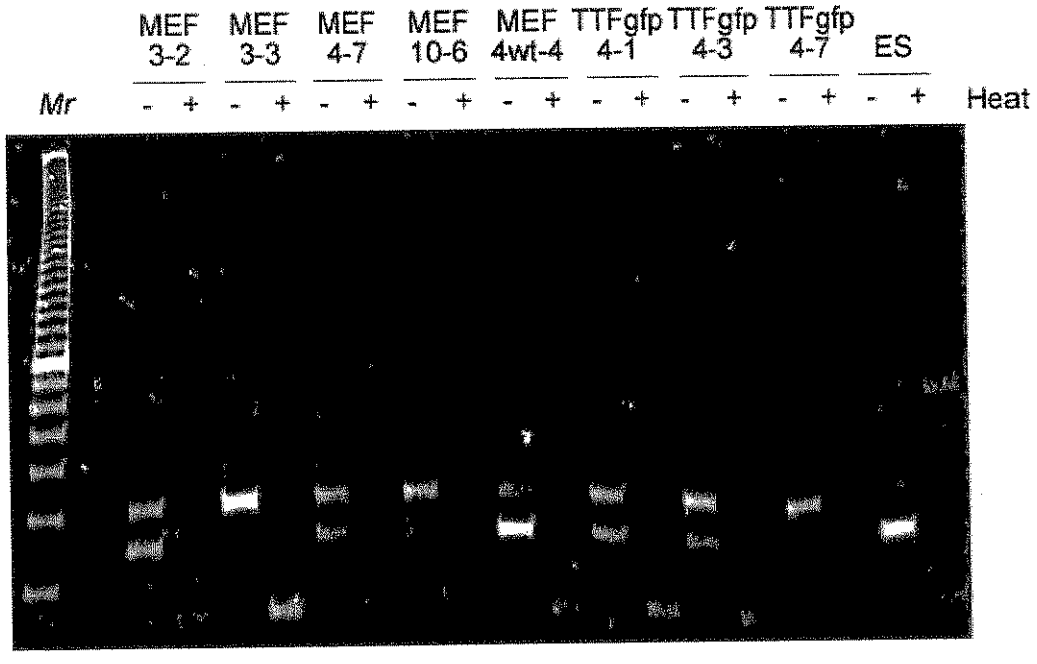

Figure S2. Telomerase Activities of the iPS Cells

The telomerase activities of the iPS cells and ES cells were determined with TRAPEZE telomerase detection kit (Chemicon) according to manufacturer's recommendation. The lysates heated at 85°C for 10 minutes were used as negative controls. Reactions were separated on non-denaturing TBE-based 12% polyacrylamide gel electrophoresis and visualized with ethidium bromide staining.

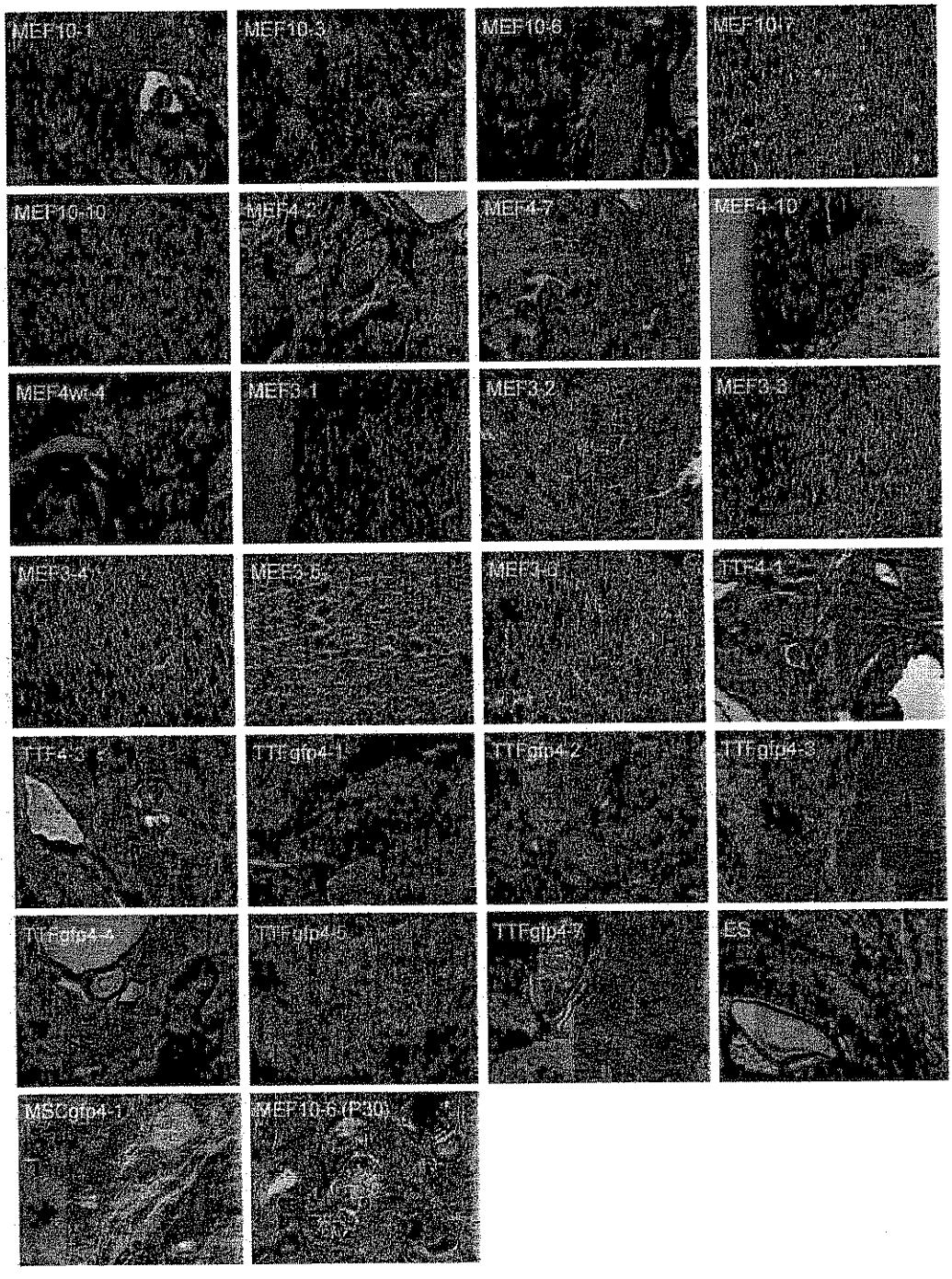

Figure S3. Histology of Teratomas

Paraffin-embedded teratomas from iPS cells were sectioned, stained with hematoxylin and eosin, and photographed with a x10 objective.

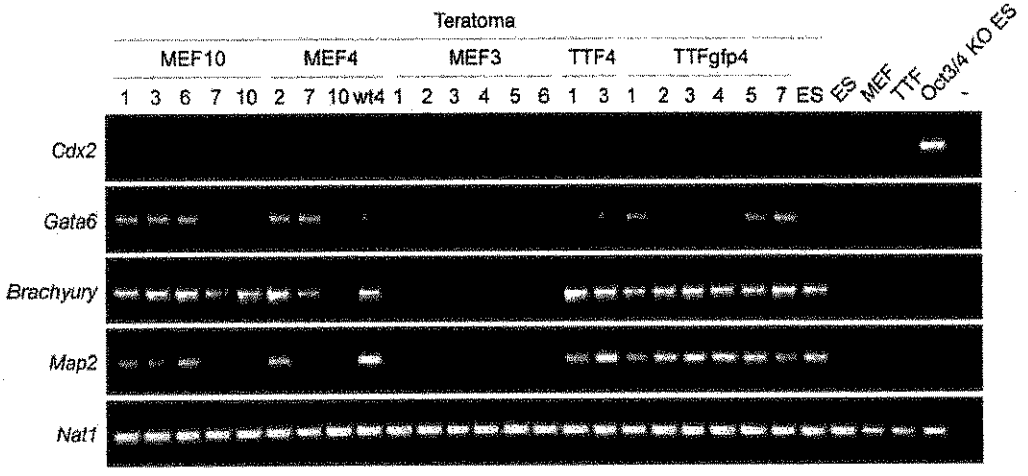

Figure S4. Expression of Marker Genes in Teratomas

We performed RT-PCR with total RNA isolated from teratomas, ES cells, MEFs, TTFs and *Oct3/4* knockout (KO) ES cells. The expression of *Cdx2* (extra-embryonic marker), *Gata6* (endoderm marker), *Brachyury* (mesoderm marker) and *Map2* (ectoderm marker) were examined. *Nat1* was used as a loading control.

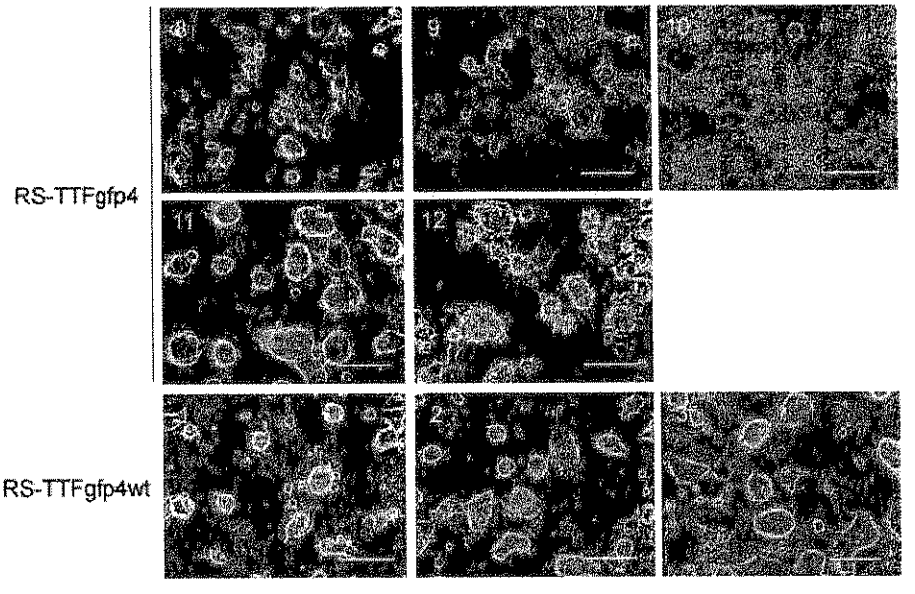

Figure S5. Morphologies of iPS Clones Derived from TTFs with the T58A Mutant (iPS-TTFgfp4-8~12) or Wild-Type c-Myc (iPS-TTFgfp4wt-1~3)

Bars indicate 200μm.

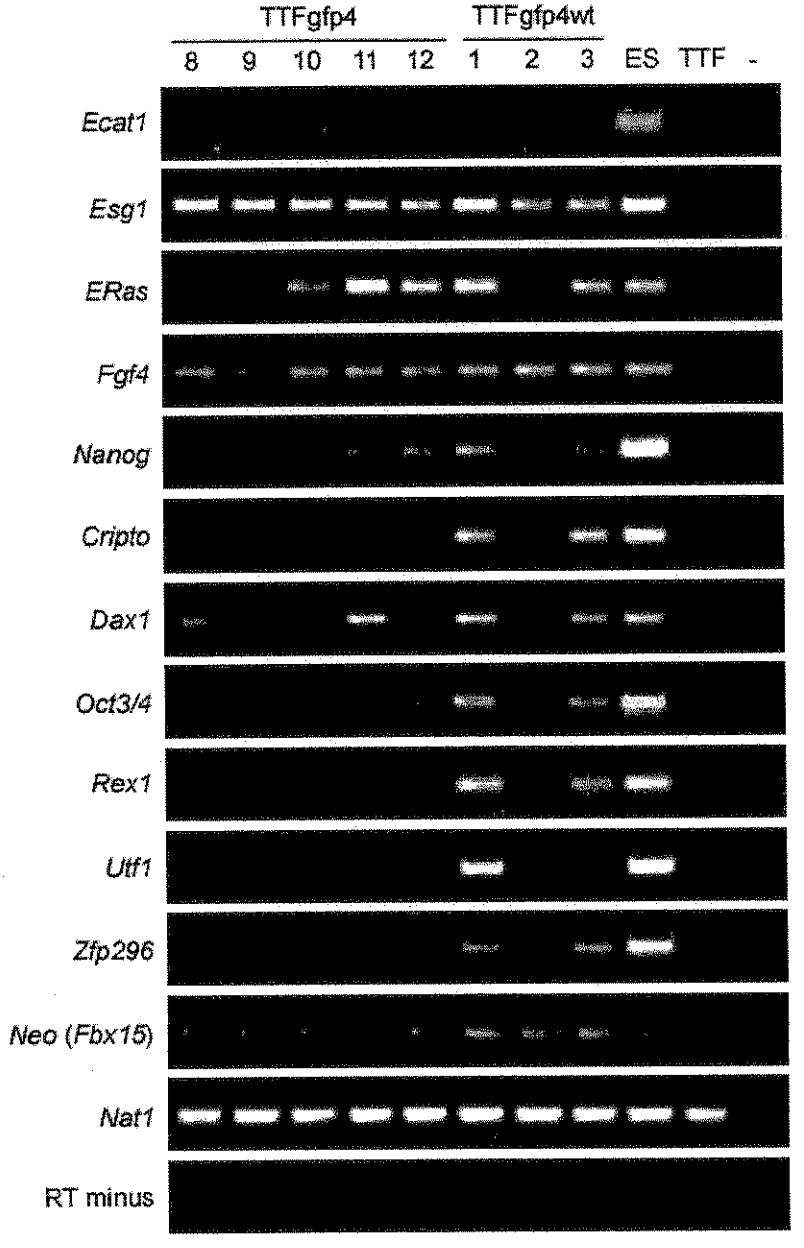

Figure S6. Expression of ES Cell Marker Genes in iPS Clones Derived from TTFs in Figure S5

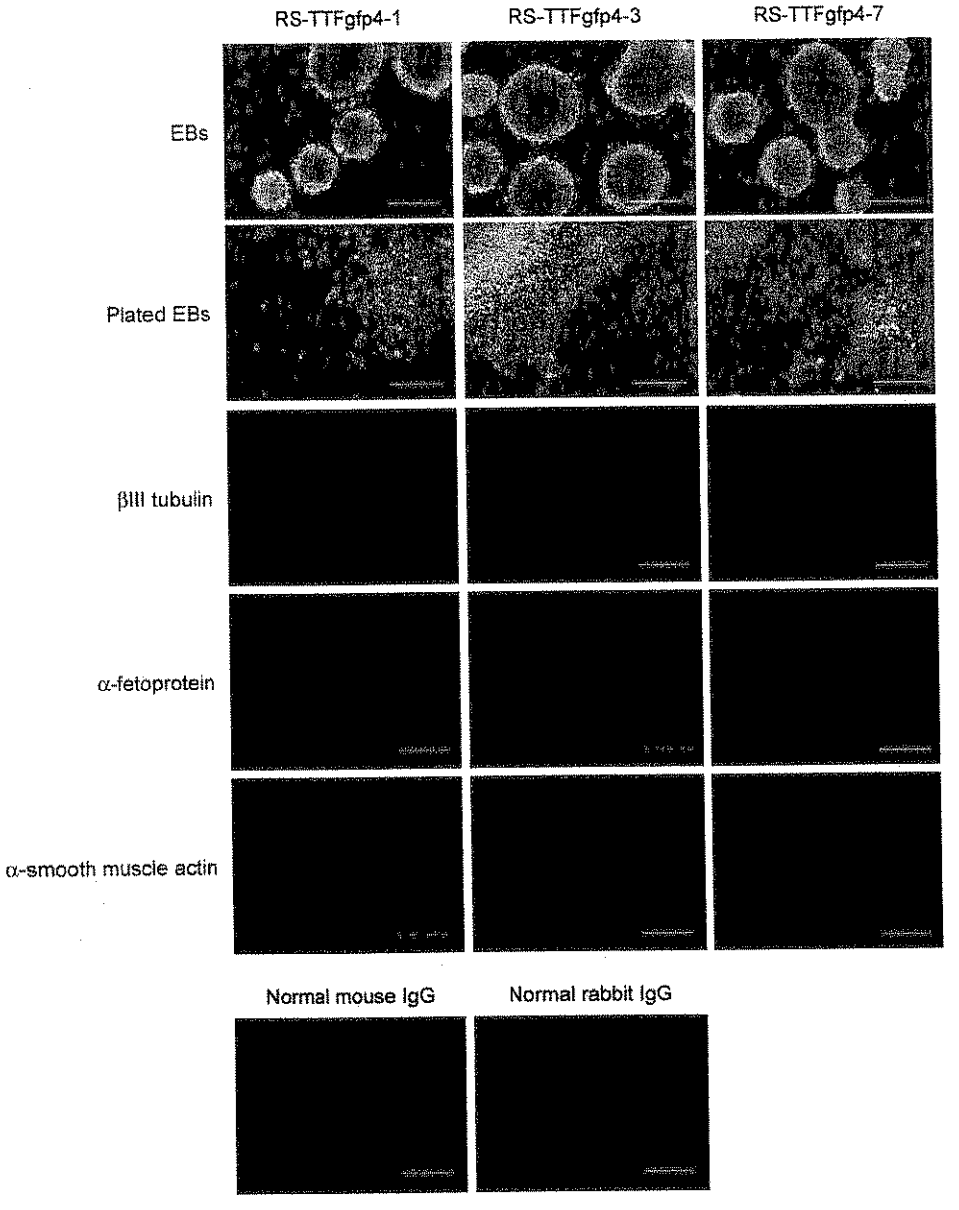

Figure S7. Pluripotency of iPS Cells Derived from Adult Tail-Tip Fibroblasts In Vitro
The iPS cells established from TTFs (iPS-TTFgfp4-1, 3 and 7) were harvested by trypsinization and plated on the bacterial culture dishes and incubated for three days in the medium without LIF. After incubation, aggregated cells were transferred to gelatin-coated tissue culture dishes and incubated another three days. Cells were then fixed and incubated with anti-βIII tubulin, anti-α-fetoprotein or anti-α -smooth muscle actin. Signals were visualized with Cy3-conjugated secondary antibody. Nucleuses were stained with DAPI. Bars indicate 200 μm. Normal mouse IgG and normal rabbit IgG antibodies were used as negative controls.

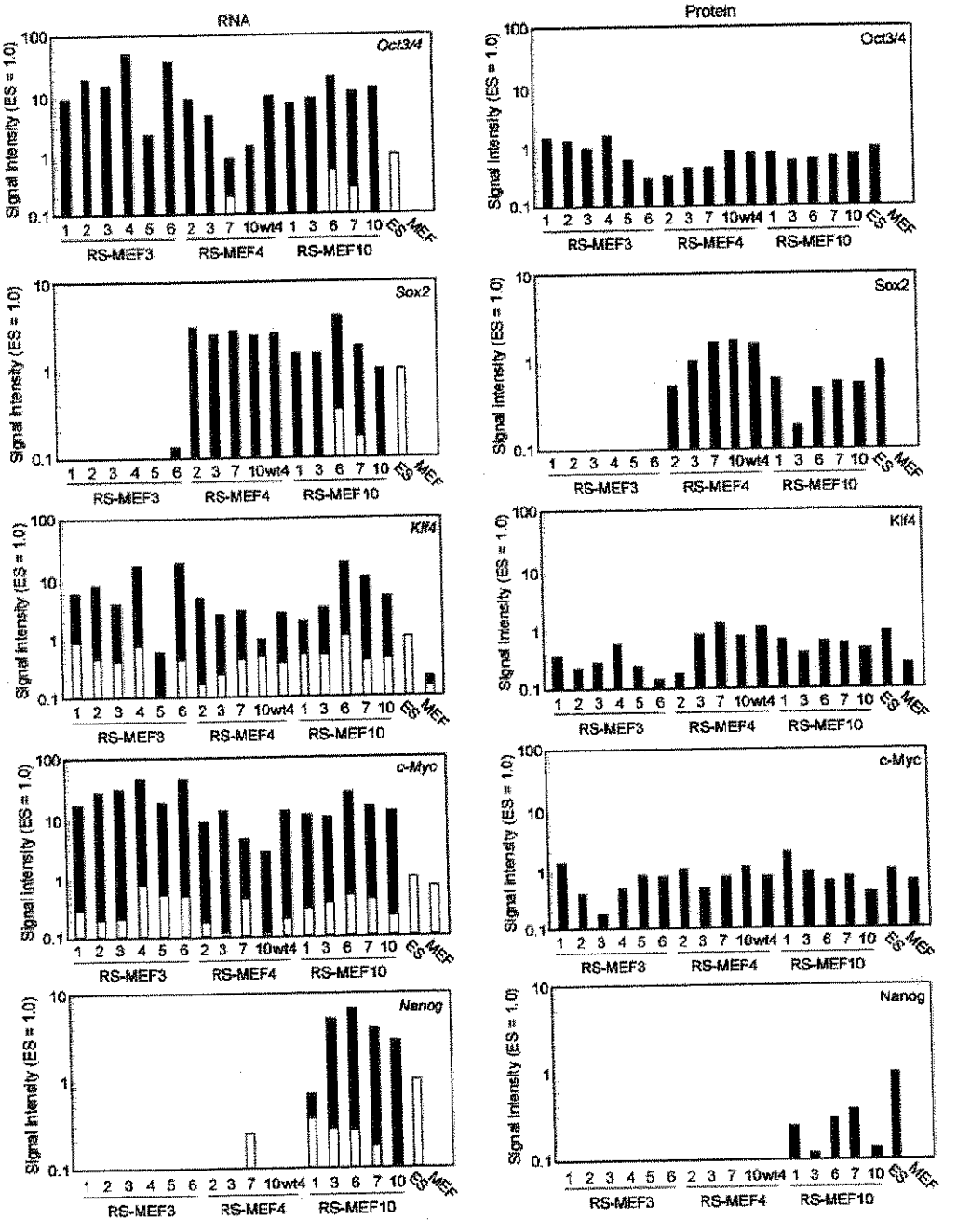

Figure S8. Quantification of RNA and Protein Levels of *Oct3/4*, *Sox2*, *Klf4*, *c-myc*, and *Nanog*

RNA levels were determine with real-time PCR with primers specific for endogenous transcripts (open column) or those common for both endogenous and transgenic transcripts (open and closed column). Protein levels were determined by Western blot and normalized with β-actin. Shown are relative expression levels compared to those in ES cells. Data of MEF are also shown.

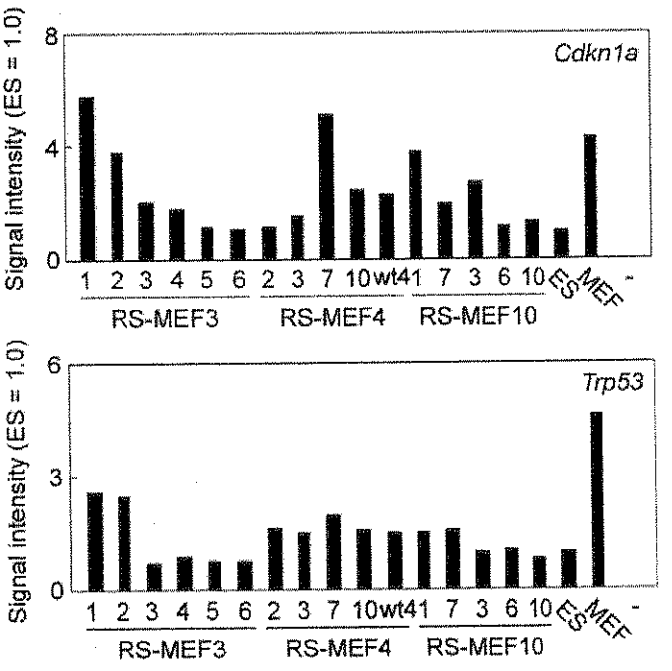

Figure S9. Expression of p53 and p21 in iPS Cells

We performed real time PCR to determine the RNA levels of p21 (*Cdkn1a*) and p53 (*Trp53*) in iPS cells, ES cells, and MEF. Shown are relative expression levels compared to those in ES cells.

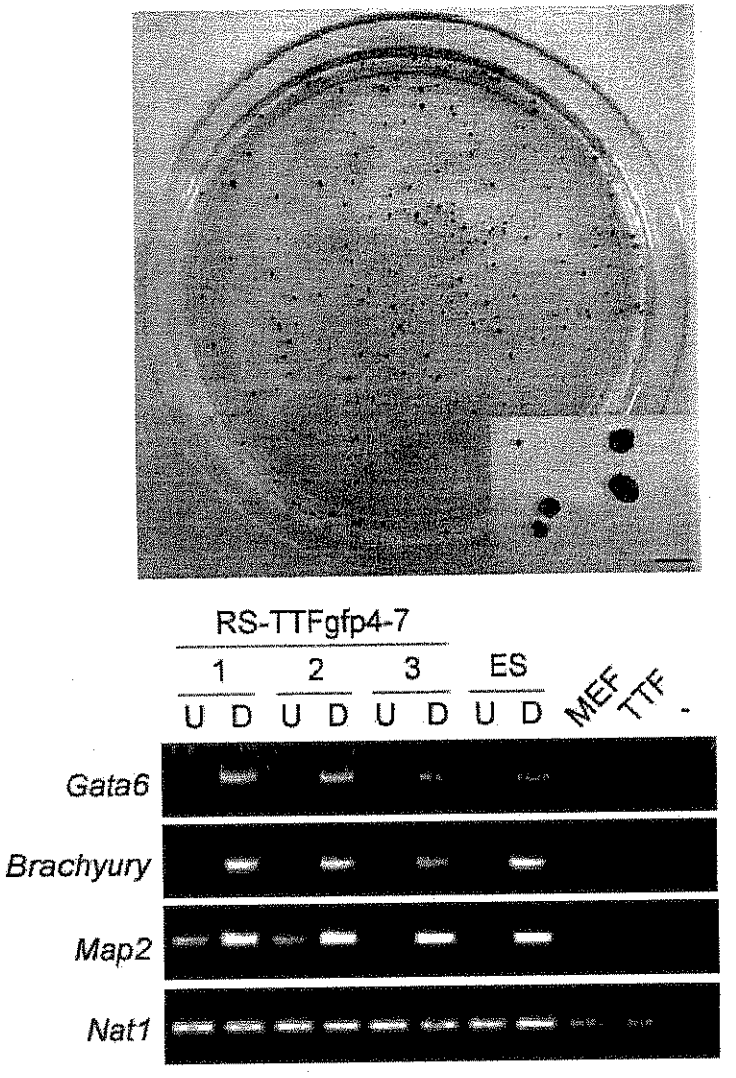

Figure S10. Clonal Analyses of iPS Cells

iPS-TTFgfp4-7 cells were plated at a clonal density (2000 cells per 100-mm dish). Seven days later, colonies were stained with alkaline phosphatase (upper). Colonies were picked and expanded for *in vitro* differentiation analysis. RT-PCR showed the each subclone can differentiate into all three germ layers (lower).

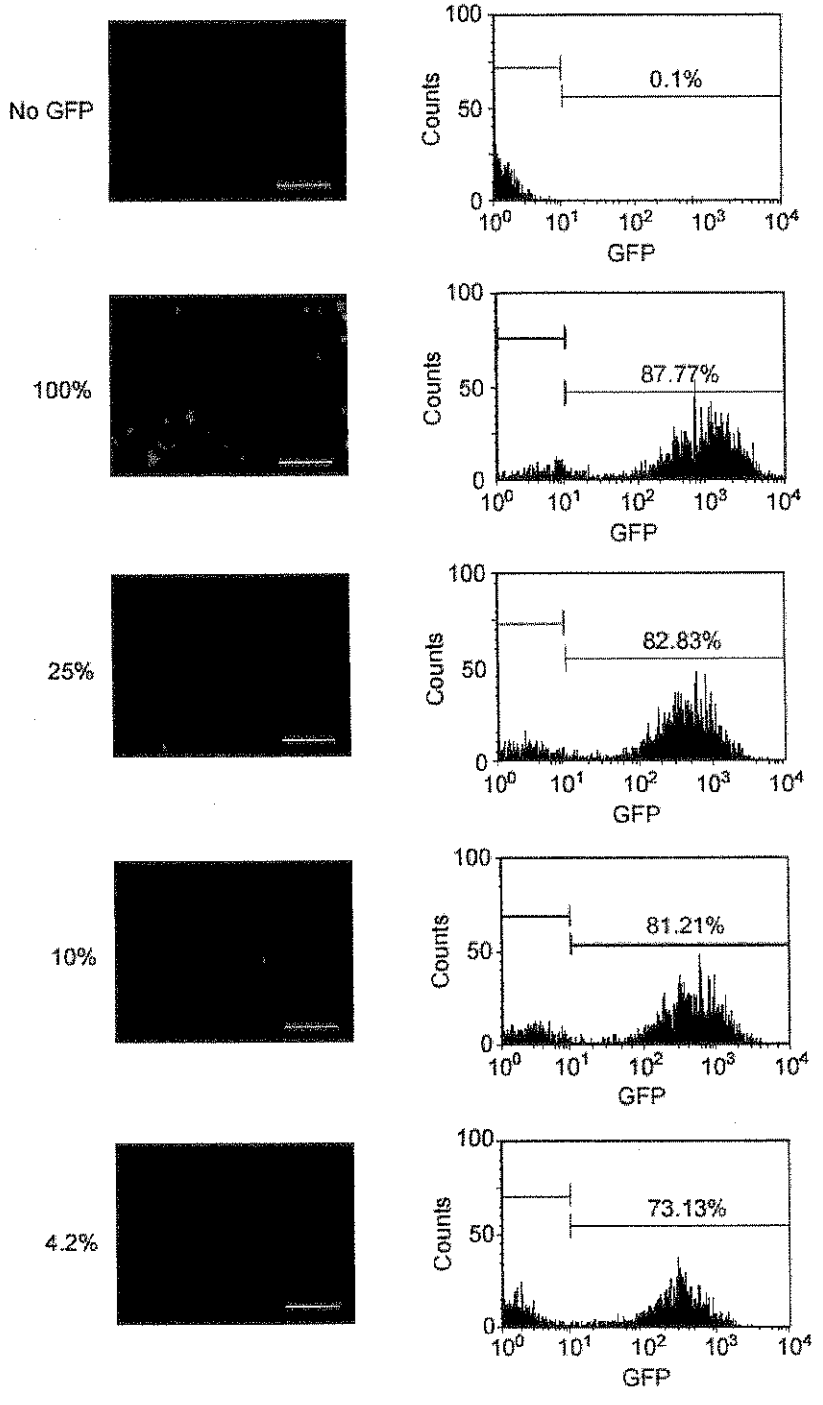

Figure S11. Transfection Efficiency of the PLAT-E Cells and pMX System

We transfected the GFP-expressing retroviral vector and the control vector at ratios of 1:0, 1:3, 1:9, and 1:23 into MEFs, with a constant amount of total DNA. Forty-eight hours later, cells were photographed under a fluorescence microscope and analyzed by flow cytometry. Bars indicate 200 μm. The analysis showed that 88, 83, 81, and 73% of transfected cells expressed GFP, the mean GFP fluorescence being weaker with decreased concentration of the GFP-expressing vector. This indicates that ~47% (0.83^4), ~12% (0.81^{10}), and ~0.05% (0.73^{24}) of cells transfected with the four, 10, or 24 factors expressed all the factors, respectively. In a 100-mm dish, we plated 8 x 10^5 cells, of which ~4 x 10^5 cells should express all the four selected factors when transfected. By contrast, we obtained ~100 iPS colonies after selection with G418 after introduction of the four factors. Thus, a small portion (~0.02%) of transfected cells becomes ES-like after introduction of the four selected factors.

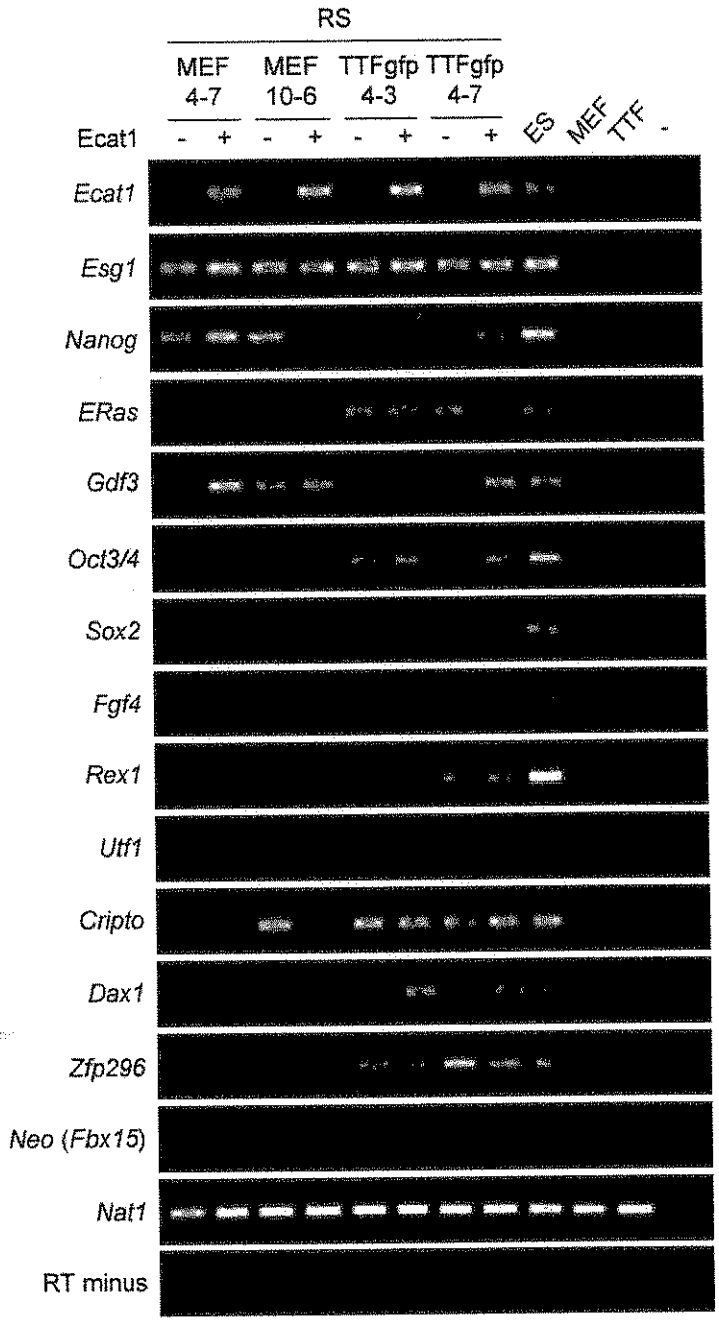

Figure S12. Effect of Forced Expression of *Ecat1* in iPS Cells on the Expression of ES Cell Marker Genes

iPS cells (iPS-MEF4-7, MEF10-6, TTFgfp4-3 and TTFgfp4-7) were transfected with pMX-IP (indicated as -) or pMX-ECAT1-IP encoding *Ecat1* (indicated as +). Forty-eight hours after infection, the cells were selected with 2 μg/ml of puromycin for 2 days to eliminate the non-infected cells. Total RNA was isolated from these cells and analyzed with RT-PCR. The effect of ECAT1 was variable. In two clones (iPS-MEF4-7, iPS-TTFgfp4-7), forced expression of ECAT1 slightly enhance the expression of *Nanog* and *Gdf3*. However, in other two clones (iPS- MEF10-6, iPS-TTFgfp4-3), ECAT1 expression decreased the expression of *Nanog*. In iPS-MEF10-6, many other genes were also suppressed by the forced expression of ECAT1. Thus, it is unlikely that ECAT1 has a strong positive effect on the induction of iPS cells.

Table S1. Symbols, Accession Numbers, and Primers for Cloning of 24 Candidate Factors

No.	Symbol	Accession	Primers for Cloning
1	Ecat1	AB211060	CAC CAT GGC ATC TCT AAA GAG GTT TCA GAC
			TTA TAA TAT GAT AAA TGA TTC CCA GGC ATC
2	Dppa5 (Esg1)	NM_025274	AAA AAG CAG GCT GGA TGA TGG TGA CCC TCG TGA
			AGA AAG CTG GGT CTG CAT CCA GGT CGG AGA CA
3	Fbxo15	NM_015798	AAA AAG CAG GCT CAA TAA TGG AGG AGT CGG AAT TGG
			AGA AAG CTG GGT CCA TTT ATT GCC TCC CAA ACC ATTG
4	Nanog	AB093574	AAA AAG CAG GCT CTG ACA TGA GTG TGG GTC TT
			AGA AAG CTG GGT AAG TCT CAT ATT TCA CCT GG
5	ERas	NM_181548	AAA AAG CAG GCT GGG GAA TGG CTT TGC CTA
			AGA AAG CTG GGT CAA AGA TCT TCA GGC TAC AG
6	Dnmt3l	NM_019448	AAA AAG CAG GCT CAA TGG GTT CCC GGG AGA CAC
			AGA AAG CTG GGT CCT GGT TCT AGG AAA GAC TT

7	Ecat8	AB211061	AAA AAG CAG GCT AGA AGG GCC AGG ATG TTC GAG GTC
			AGA AAG CTG GGT GTT GGA AAG GGC TGG CAT GTC GT
8	Gdf3	NM_008108	AAA AAG CAG GCT CGA CCA TGC AGC CTT ATC AAC G
			AGA AAG CTG GGT ACA CTC CTA GCC TAG TCC CGA GAC
9	Sox15	NM_009235	CAC CAT GGC GCT GAC CAG CTC CTC ACA A
			TTA AAG GTG GGT TAC TGG CAT GGG
10	Dppa4	NM_028610	CAC CAT GGA GAC TGC TGG AGA CAA GAA G
			TTA TCC TTC GAG GCT CTT AGT CAA
11	Dppa2	NM_028615	CAC CAT GTC ATA CTT CGG CCT GGA GAC T
			TGT CTA CGG CGG CAT ATT TGG GGG
12	Fthl17	NM_031261	CAC CAT GGC CGA AGC GCC CTC TCG AGT G
			TTA GGA CAG GCT GAG CTT GTC AAA GAG G
13	Sall4	NM_175303	CAC CAT GTC GAG GCG CAA GCA GGC GAA GCC
			TTA GCT GAC AGC AAT CTT ATT TTC CTC CAG

14	Oct3/4 (Pou5f1)	NM_013633	AAA AAG CAG GCT CCA CCT TCC CCA TGG CTG GAC ACC
			AGA AAG CTG GGT TGA TCA ACA GCA TCA CTG AGC TTC
15	Sox2	NM_011443	AAA AAG CAG GCT TGT ATA ACA TGA TGG AGA CGG
			AGA AAG CTG GGT TTC ACA TGT GCG ACA GGG GCA GT
16	Rex1 (Zfp42)	NM_009556	CAC CGA CAA CAT GAA TGA ACA AAA A
			CAA TCT GTC TCC ACC TTC AGC ATT T
17	Utf1	NM_009482	CAC CCC TCT ACC TGG CTC AGG GAT G
			ACA AAG CTT TAT TGG CGC AAG TCC C
18	Tcl1	NM_009337	CAC CAT GGC TAC CCA GCG GGC ACA CA
			TTA TTC ATC GTT GGA CTC CGA GTC TAT CAG
19	Dppa3 (Stella)	NM_139218	CAC CAT GGA GGA ACC ATC AGA GAA AGT C
			CTA ATT CTT CCC GAT TTT CGC ATT CT
20	Klf4	NM_010637	CAC CAT GGC TGT CAG CGA CGC TCT GCT C
			ACA TCC ACT ACG TGG GAT TTA AAA

21	β-catenin	NM_007614	CAC CAT GGC TAC TCA AGC TGA CCT GAT GG
			GCT TTC TTA CCT AAA GGA CGA TTT ACA GGT C
22	c-Myc	NM_010849	CAC CAT GCC CCT CAA CGT GAA CTT CAC C
			TTA TGC ACC AGA GTT TCG AAG CTG TTC G
23	Stat3	NM_213659	AAA AAG CAG GCT CCA GGA TGG CTC AGT GGA ACC AG
			AGA AAG CTG GGT CAC ATG GGG GAG GTA GCA CAC
24	Grb2	NM_008163	AAA AAG CAG GCT TCA TCC CCA AGA ATT ACA T
			AGA AAG CTG GGT CTT AGA GCG CCT GGA CGT AG

Table S2. List of Transfection Experiments in This Study

Date	Cells	Transgenes	G418-Resistant Colonies	Colonies Picked up	iPS Clones Established
7/19/2005	MEF 1×10^5	Mock	0		
		Ecat1	0		
		Esg1	0		
		Fbx15	0		
		Nanog	0		
		ERas	0		
		Dnmt3l	0		
		Ecat8	0		
		Gdf3	0		
		Sox15	0		
		Dppa4	0		
		Dppa2	0		
		Fthl17	0		
		Sall4	0		
		Oct3/4	0		
		Sox2	0		
		Rex1	0		
		Utf1	0		
		Tcl1	0		
		Dppa3	0		
		Klf4	0		

		β-catenin S33Y	0		
		Myc T58A	0		
		Stat3-C	0		
		Grb2 ΔSH2	0		
		24 factors	22	12	5 MEF24-1-4 MEF24-1-5 MEF24-1-9 MEF24-1-17 MEF24-1-18
8/15/2005	MEF 1 x 10^5	Mock	0		
		24 factors	29	6	4 MEF24-2-1 ~4
8/29/2005	MEF 1 x 10^5	Mock	0		
		24 factors – Ecat1	2	1	frozen in 24-well plate
		24 factors – Esg1	22	1	
		24 factors – Fbx15	10	1	
		24 factors – Nanog	5	1	
		24 factors – ERas	9	1	
		24 factors – Dnmt3l	22	1	
		24 factors – Ecat8	19	1	
		24 factors – Gdf3	9	1	
		24 factors – Sox15	30	1	
		24 factors – Dppa4	17	1	

		24 factors – Dppa2	9	1	
		24 factors – Fthl17	5	1	
		24 factors – Sall4	17	1	
		24 factors – Oct3/4	0		
		24 factors – Sox2	0		
		24 factors – Rex1	15	1	frozen in 24-well plate
		24 factors – Utf1	8	1	
		24 factors – Tcl1	4	1	
		24 factors – Dppa3	7	1	
		24 factors – Klf4	0		
		24 factors – β-catenin S33Y	15	1	frozen in 24-well plate
		24 factors – Myc T58A	4	1	
		24 factors – Stat3-C	22	1	
		24 factors – Grb2 ΔSH2	11	1	
		24 factors	22	1	
9/12/2005	MEF 8×10^5	Mock	0		
		10 factors – Fbx15	183	2	frozen in 24-well plate
		10 factors – Nanog	170	2	
		10 factors – ERas	146	2	
		10 factors – Dppa2	177	2	
		10 factors – Oct3/4	0		
		10 factors – Sox2	5	2	frozen in 24-well plate
		10 factors – Tcl1	206	2	
		10 factors – Klf4	0		

		10 factors −β-catenin S33Y	129	2	frozen in 24-well plate
		10 factors − Myc T58A	46	2	
		10 factors	176	2	
		24 factors	28	2	
9/26/2005	MEF 8×10^5	Mock	0		
		4 factors	160	12	3 MEF4-2, MEF4-3, MEF4-7, MEF4-10
		4 factors − Myc T58A	36	6	
		4 factors − Klf4	1	1	
		4 factors − Sox2	54	6	6 MEF3-1 -6
		4 factors − Oct3/4	1	1	
		Oct3/4 +Sox2	0		
		Oct3/4 +Klf4	0		
		Oct3/4 +Myc T58A	0		
		Sox2 +Klf4	0		
		Sox2 +Myc T58A	0		
		Klf4 +Myc T58A	0		

		10 factors	179	12	5 MEF10-1, MEF10-3, MEF10-6, MEF10-7, MEF10-10
11/14/2005	TTF 8×10^5	GFP	0		
		4 factors	3	3	3 TTF4-1 ~3
		10 factors	39	12	12 TTF10-1 ~12
	MSC 8×10^5	GFP	0		
		4 factors	3	3	3 MSC4-1 ~3
		10 factors	0		
11/20/2005	MEF 8×10^5	GFP	0		
		4 factors (Myc wt)	43	6	4 MEF4wt-1 MEF4wt-3 MEF4wt-4 MEF4wt-6
		4 factors (Myc T58A)	35	6	6 MEF4-13 ~18
		4 factors – Myc	0		

12/29/2005	TTFgfp 8 x 10^5	Mock	0		
		4 factors	13	6	6 TTFgfp4-1 ~6
		4 factors (flox)	3	3	1 TTFgfp4-7
		10 factors	17	3	1 TTFgfp10-1
	MSCgfp 8 x 10^5	Mock	0		
		4 factors	3	3	1 MSCgfp-1
		10 factors	0		
4/11/2006	TTFgfp 8 x 10^5	Mock	0		
		4 factors (Myc wt)	3	3	3 TTFgfp4wt1 ~3
		4 factors (Myc T58A)	5	5	5 TTFgfp4-8 ~12

Table S3. Genes Belonging to Group I in Figure 4B

Genbank	Description
AK045520;XM_130148	Mus musculus cDNA clone MGC:102197 IMAGE:5716088, complete cds. [BC085507]
NM_012054	Mus musculus acyloxyacyl hydrolase (Aoah), mRNA [NM_012054]
NM_144912.1;NM_144912	Mus musculus RAD9 homolog B (S. cerevisiae) (Rad9b), mRNA [NM_144912]
NM_008635	Mus musculus microtubule-associated protein 7 (Mtap7), mRNA [NM_008635]
NM_026477;NM_144953	Mus musculus RIKEN cDNA 1700019D03 gene (1700019D03Rik), mRNA [NM_144953]
AK010400;NM_212457	Mus musculus brain expressed, X-linked 4 (Bex4), mRNA [NM_212457]
NM_011973	Mus musculus renal tumor antigen (Rage), mRNA [NM_011973]
AK049376;	Mus musculus ES cells cDNA, RIKEN full-length enriched library, clone:C330038P18 product:heterogeneous nuclear ribonucleoprotein U, full insert sequence [AK049375]
NM_013840	Mus musculus ubiquitously expressed transcript (Uxt), mRNA [NM_013840]
NM_029554	Mus musculus RIKEN cDNA 0610040J01 gene (0610040J01Rik), mRNA [NM_029554]
AK010559;XM_112612	Mus musculus ES cells cDNA, RIKEN full-length enriched library, clone:2410019P08 product:hypothetical Proline-rich region/Zinc finger, C2H2 type containing protein, full insert sequence. [AK010559]
NM_025533	Mus musculus nitric oxide synthase interacting protein (Nosip), mRNA [NM_025533]
NM_134251	Mus musculus solute carrier family 12 (potassium/chloride transporters), member 8 (Slc12a8), mRNA [NM_134251]
NM_008532	Mus musculus tumor-associated calcium signal transducer 1 (Tacstd1), mRNA [NM_008532]
AK045412;XM_136135	Mus musculus 11 days pregnant adult female ovary and uterus cDNA, RIKEN full-length enriched library, clone:5031428K02 product:similar to CDNA FLJ14503 FIS, CLONE NT2RM1000252, WEAKLY SIMILAR TO H.SAPIENS E-MAP-115 MRNA [Homo sapiens], full insert sequence. [AK030316]
NM_026323	Mus musculus WAP four-disulfide core domain 2 (Wfdc2), mRNA [NM_026323]

NM_007957	Mus musculus extraembryonic, spermatogenesis, homeobox 1 (Esx1), mRNA [NM_007957]
NM_008822	Mus musculus peroxisome biogenesis factor 7 (Pex7), mRNA [NM_008822]
AB021860;NM_013924	Mus musculus activator of basal transcription (Abt1), mRNA [NM_013924]
NM_030722	Mus musculus pumilio 1 (Drosophila) (Pum1), mRNA [NM_030722]
AK075793;NM_026468	Mus musculus ATP synthase, H+transporting, mitochondrial F0 complex, subunit c (subunit 9), isoform 2 (Atp5g2), mRNA [NM_026468]
NM_021397	Mus musculus repressor of GATA (Rog), mRNA [NM_021397]
AK051480;NM_172293	Mus musculus hypothetical protein MGC47262 (MGC47262), mRNA [NM_172293]
AK005720;	Mus musculus adult male testis cDNA, RIKEN full-length enriched library, clone:1700007J06 product:hypothetical RNI-like structure containing protein, full insert sequence. [AK005720]
AK004470;	Mus musculus 18-day embryo whole body cDNA, RIKEN full-length enriched library, clone:1190003J15 product:hypothetical protein, full insert sequence. [AK004470]
AK019664;	Mus musculus adult male testis cDNA, RIKEN full-length enriched library, clone:4930502N02 product:hypothetical Adenylate kinase/Glutamic acid-rich region containing protein, full insert sequence. [AK019664]
NM_133945	Mus musculus vaccinia related kinase 3 (Vrk3), mRNA [NM_133945]
AK016103;NM_026301	Mus musculus ring finger protein 125 (Rnf125), mRNA [NM_026301]
BC018510;	Mus musculus cDNA sequence BC018510, mRNA (cDNA clone MGC:6783 IMAGE:2645293), complete cds. [BC018510]
NM_009514	Mus musculus pre-B lymphocyte gene 3 (Vpreb3), mRNA [NM_009514]
NM_033597	Mus musculus myeloblastosis oncogene (Myb), mRNA [NM_033597]
BC011109;NM_029649	Mus musculus RIKEN cDNA 2610511E22 gene (2610511E22Rik), mRNA [NM_029649]
NM_021099	Mus musculus kit oncogene (Kit), mRNA [NM_021099]
NM_010361	Mus musculus glutathione S-transferase, theta 2 (Gstt2), mRNA [NM_010361]
NM_019472	Mus musculus myosin X (Myo10), mRNA [NM_019472]

NM_053071	Mus musculus cytochrome c oxidase, subunit VIc (Cox6c), mRNA [NM_053071]
BC004728;NM_174992	Mus musculus cDNA sequence BC004728 (BC004728), mRNA [NM_174992]
NM_008860	Mus musculus protein kinase C, zeta (Prkcz), mRNA [NM_008860]
NM_011884	Mus musculus RNA guanylyltransferase and 5'-phosphatase (Rngtt), mRNA [NM_011884]
NM_011305	Mus musculus retinoid X receptor alpha (Rxra), mRNA [NM_011305]
NM_022985	Mus musculus zinc finger, A20 domain containing 3 (Za20d3), mRNA [NM_022985]
NM_007507	Mus musculus ATP synthase, H+transporting, mitochondrial F1F0 complex, subunit e (Atp5k), mRNA [NM_007507]
AK045266;XM_484570	Mus musculus splicing factor, arginine/serine-rich 15, mRNA (cDNA clone MGC:67163 IMAGE:6417362), complete cds. [BC057592]
AA050368;NM_001017429	Mus musculus cytochrome c oxidase, subunit XVII assembly protein homolog (yeast) (Cox17), mRNA [NM_001017429]
NM_026068	Mus musculus mediator of RNA polymerase II transcription, subunit 31 homolog (yeast) (Med31), mRNA [NM_026068]
NM_013769	Mus musculus tight junction protein 3 (Tjp3), mRNA [NM_013769]
NM_008595	Mus musculus manic fringe homolog (Drosophila) (Mfng), mRNA [NM_008595]
NM_013892	Mus musculus proprotein convertase subtilisin/kexin type 1 inhibitor (Pcsk1n), mRNA [NM_013892]
NM_028661	Mus musculus RIKEN cDNA 1110006G06 gene (1110006G06Rik), mRNA [NM_028661]
NM_008108	Mus musculus growth differentiation factor 3 (Gdf3), mRNA [NM_008108]
NM_009342	Mus musculus t-complex testis expressed 1 (Tctex1), mRNA [NM_009342]
AK033656;NM_153062	Mus musculus solute carrier family 37 (glycerol-3-phosphate transporter), member 1 (Slc37a1), mRNA [NM_153062]
AK031494;XM_619899	Mus musculus 13 days embryo male testis cDNA, RIKEN full-length enriched library, clone:6030440P17 product:hypothetical protein, full insert sequence. [AK031494]

NM_013633	Mus musculus POU domain, class 5, transcription factor 1 (Pou5f1), mRNA [NM_013633]
NM_025838	Mus musculus RIKEN cDNA 1110004B13 gene (1110004B13Rik), mRNA [NM_025838]
AF176530;	Mus musculus F-box protein FBX15 mRNA, partial cds. [AF176530]
AK038557;NM_178739	Mus musculus WD repeat domain 40B (Wdr40b), mRNA [NM_178739]
NM_009575	Mus musculus zinc finger protein of the cerebellum 3 (Zic3), mRNA [NM_009575]
AK045292;XM_619147	PREDICTED: Mus musculus methylcrotonoyl-Coenzyme A carboxylase 2 (beta) (Mccc2), mRNA [XM_127493]
NM_022024	Mus musculus glia maturation factor, gamma (Gmfg), mRNA [NM_022024]
NM_021480	Mus musculus L-threonine dehydrogenase (Tdh), mRNA [NM_021480]
NM_013545	Mus musculus hemopoietic cell phosphatase (Hcph), mRNA [NM_013545]
AK032336;NM_153508	Mus musculus calsyntenin 3 (Clstn3), mRNA [NM_153508]
AB042155;NM_022987	Mus musculus zinc finger protein of the cerebellum 5 (Zic5), mRNA [NM_022987]
NM_007430	Mus musculus nuclear receptor subfamily 0, group B, member 1 (Nr0b1), mRNA [NM_007430]

Table S4. Genes Belonging to Group II in Figure 4B

Genbank	Description
AK077630;NM_172670	Mus musculus glycosyltransferase-like 1B (Gyltl1b), mRNA [NM_172670]
NM_030676	Mus musculus nuclear receptor subfamily 5, group A, member 2 (Nr5a2), mRNA [NM_030676]
NM_007866	Mus musculus delta-like 3 (Drosophila) (Dll3), transcript variant 1, mRNA [NM_007866]
NM_024440	Mus musculus Der1-like domain family, member 3 (Derl3), mRNA [NM_024440]
AK009303;NM_027366	Mus musculus lymphocyte antigen 6 complex, locus G6E (Ly6g6e), mRNA [NM_027366]
NM_029948	Mus musculus RIKEN cDNA 4930569K13 gene (4930569K13Rik), mRNA [NM_029948]
NM_008955	Mus musculus placenta specific homeobox 1 (Psx1), mRNA [NM_008955]
NM_023755	Mus musculus transcription factor CP2-like 1 (Tcfcp2l1), mRNA [NM_023755]
NM_010168	Mus musculus coagulation factor II (F2), mRNA [NM_010168]
NM_009236	Mus musculus SRY-box containing gene 18 (Sox18), mRNA [NM_009236]
AK015697;XM_126856	Mus musculus adult male testis cDNA, RIKEN full-length enriched library, clone:4930504H06 product:hypothetical EF-hand structure containing protein, full insert sequence. [AK015697]
AK049153;NM_172283	Mus musculus fucokinase (Fuk), transcript variant 1, mRNA [NM_172283]
AK032023;NM_172994	Mus musculus protein phosphatase 2 (formerly 2A), regulatory subunit B (PR 52), gamma isoform (Ppp2r2c), mRNA [NM_172994]
AK017618;NM_175238	Mus musculus Rap1 interacting factor 1 homolog (yeast) (Rif1), mRNA [NM_175238]
NM_010014	Mus musculus disabled homolog 1 (Drosophila) (Dab1), mRNA [NM_010014]
AK006101;	Mus musculus adult male testis cDNA, RIKEN full-length enriched library, clone:1700019A02 product:hypothetical Glutamic acid-rich region containing protein, full insert sequence. [AK006101]
NM_011635	Mus musculus tumor rejection antigen P1A (Trap1a), mRNA [NM_011635]
AK002979;	Mus musculus adult male brain cDNA, RIKEN full-length enriched library, clone:0710001P07 product:similar to D1 DOPAMINE RECEPTOR-INTERACTING PROTEIN CALCYON [Homo

	sapiens], full insert sequence. [AK002979]
AK052256;NM_011934	Mus musculus estrogen related receptor, beta (Esrrb), mRNA [NM_011934]
NM_009556	Mus musculus zinc finger protein 42 (Zfp42), mRNA [NM_009556]
AK003211;XM_356184	PREDICTED: Mus musculus RIKEN cDNA 1110001D15 gene (1110001D15Rik), mRNA [XM_356184]
NM_013873;	Mus musculus sulfotransferase-related protein (Sultx3) mRNA, complete cds. [AF059257]
AK049114;NM_175342	Mus musculus RIKEN cDNA C330003B14 gene (C330003B14Rik), mRNA [NM_175342]
AY069926;NM_145464	Mus musculus SRY-box containing gene 21 (Sox21), mRNA [NM_145464]
NM_011401	Mus musculus solute carrier family 2 (facilitated glucose transporter), member 3 (Slc2a3), mRNA [NM_011401]
BC016190;NM_029794	Mus musculus DNA segment, Chr 11, ERATO Doi 636, expressed (D11Ertd636e), mRNA [NM_029794]
NM_009646	Mus musculus autoimmune regulator (autoimmune polyendocrinopathy candidiasis ectodermal dystrophy) (Aire), mRNA [NM_009646]
AK030701;NM_177591	Mus musculus immunoglobulin superfamily, member 1 (Igsf1), transcript variant 1, mRNA [NM_177591]
NM_029395.1;	Mus musculus 8 days embryo whole body cDNA, RIKEN full-length enriched library, clone:5730441M18 product:hypothetical Zinc finger, C2H2 type containing protein, full insert sequence. [AK017633]
AK033197;NM_028610	Mus musculus developmental pluripotency associated 4 (Dppa4), transcript variant 1, mRNA [NM_028610]
NM_023894	Mus musculus placenta specific homeobox 2 (Psx2), mRNA [NM_023894]
NM_025274	Mus musculus developmental pluripotency associated 5 (Dppa5), mRNA [NM_025274]
AK010816;XM_203409	PREDICTED: Mus musculus nuclear domain 10 protein 52 (Ndp52), mRNA [XM_203409]
AK035177;NM_178367	Mus musculus DEAH (Asp-Glu-Ala-His) box polypeptide 33 (Dhx33), mRNA [NM_178367]

NM_008501	Mus musculus leukemia inhibitory factor (Lif), mRNA [NM_008501]
NM_026480	Mus musculus RIKEN cDNA 2410146L05 gene (2410146L05Rik), mRNA [NM_026480]
AK010332;XM_132755	Mus musculus mRNA for homeobox transcription factor Nanog, complete cds. [AB093574]
NM_008614	Mus musculus myelin-associated oligodendrocytic basic protein (Mobp), mRNA [NM_008614]
NM_019743	Mus musculus RING1 and YY1 binding protein (Rybp), mRNA [NM_019743]
NM_011443	Mus musculus SRY-box containing gene 2 (Sox2), mRNA [NM_011443]
AK028078;XM_140052	PREDICTED: Mus musculus RIKEN cDNA 1700061G19 gene (1700061G19Rik), mRNA [XM_140052]
AK049997;NM_144518	Mus musculus RIKEN cDNA 2900011O08 gene (2900011O08Rik), mRNA [NM_144518]
AK077033;NM_172799	Mus musculus RIKEN cDNA 4932418K24 gene (4932418K24Rik), mRNA [NM_172799]
NM_011328	Mus musculus secretin (Sct), mRNA [NM_011328]
NM_023508	Mus musculus phosducin-like 2 (Pdcl2), mRNA [NM_023508]
NM_023219	Mus musculus solute carrier family 5 (neutral amino acid transporters, system A), member 4b (Slc5a4b), mRNA [NM_023219]
AK036673;NM_175482	Mus musculus ubiquitin specific protease 28 (Usp28), mRNA [NM_175482]
NM_054085	Mus musculus alpha-kinase 3 (Alpk3), mRNA [NM_054085]
NM_015766	Mus musculus Epstein-Barr virus induced gene 3 (Ebi3), mRNA [NM_015766]
NM_029341	Mus musculus RIKEN cDNA 1700028N11 gene (1700028N11Rik), mRNA [NM_029341]
NM_019945	Mus musculus microtubule associated serine/threonine kinase 1 (Mast1), mRNA [NM_019945]
AY082485;NM_139218	Mus musculus developmental pluripotency-associated 3 (Dppa3), mRNA [NM_139218]
BC031460;NM_026904	Mus musculus anaphase promoting complex subunit 10 (Anapc10), mRNA [NM_026904]
AK011413;NM_031188	Mus musculus major urinary protein 1 (Mup1), mRNA [NM_031188]
NM_010262	Mus musculus gastrulation brain homeobox 2 (Gbx2), mRNA [NM_010262]
NM_009696	Mus musculus apolipoprotein E (Apoe), mRNA [NM_009696]
U60881;NM_007491	Mus musculus ADP-ribosyltransferase 5 (Art5), mRNA [NM_007491]

AB006361;NM_008963	Mus musculus prostaglandin D2 synthase (brain) (Ptgds), mRNA [NM_008963]
NM_011776	Mus musculus zona pellucida glycoprotein 3 (Zp3), mRNA [NM_011776]
NM_009133	Mus musculus stathmin-like 3 (Stmn3), mRNA [NM_009133]
NM_028783.2;NM_028783	Mus musculus roundabout homolog 4 (Drosophila) (Robo4), mRNA [NM_028783]
NM_017461	Mus musculus septin 1 (Sept1), mRNA [NM_017461]

Table S5. Genes Belonging to Group III in Figure 4B

Genbank	Description
NM_016810	Mus musculus golgi SNAP receptor complex member 1 (Gosr1), mRNA [NM_016810]
NM_020572	Mus musculus aurora kinase C (Aurkc), mRNA [NM_020572]
AK017096;XM_127023	Mus musculus adult male testis cDNA, RIKEN full-length enriched library, clone:4933437F05 product:hypothetical NAD(P)-binding Rossmann-fold domains structure containing protein, full insert sequence. [AK017096]
NM_007919	Mus musculus elastase 2 (Ela2), mRNA [NM_007919]
NM_027622	Mus musculus RIKEN cDNA 4921530G04 gene (4921530G04Rik), mRNA [NM_027622]
AK040991;XM_130488	PREDICTED: Mus musculus RIKEN cDNA A530057A03 gene (A530057A03Rik), mRNA [XM_130488]
AK010434;NM_019448	Mus musculus DNA (cytosine-5-)-methyltransferase 3-like (Dnmt3l), mRNA [NM_019448]
NM_016688	Mus musculus programmed cell death protein 7 (Pdcd7), mRNA [NM_016688]
NM_007493	Mus musculus asialoglycoprotein receptor 2 (Asgr2), mRNA [NM_007493]
NM_011060	Mus musculus peptidyl arginine deiminase, type III (Padi3), mRNA [NM_011060]
AK016694;	Mus musculus adult male testis cDNA, RIKEN full-length enriched library, clone:4933406J07 product:hypothetical protein, full insert sequence. [AK016694]
AF182945;NM_009235	Mus musculus SRY-box containing gene 15 (Sox15), mRNA [NM_009235]
NM_010758	Mus musculus myelin-associated glycoprotein (Mag), mRNA [NM_010758]
NM_019981	Mus musculus testis expressed gene 101 (Tex101), mRNA [NM_019981]
NM_007741	Mus musculus procollagen, type IX, alpha 2 (Col9a2), mRNA [NM_007741]
NM_133686	Mus musculus quinolinate phosphoribosyltransferase (Qprt), mRNA [NM_133686]
AK011820;NM_025995	Mus musculus F-box only protein 5 (Fbxo5), mRNA [NM_025995]
NM_018776	Mus musculus cytokine receptor-like factor 3 (Crlf3), mRNA [NM_018776]
NM_028937	Mus musculus RIKEN cDNA 4933406N12 gene (4933406N12Rik), mRNA [NM_028937]

NM_023587	Mus musculus protein tyrosine phosphatase-like (proline instead of catalytic arginine), member b (Ptplb), mRNA [NM_023587]
AK014932;NM_001002894	Mus musculus RIKEN cDNA 4921520L01 gene (4921520L01Rik), mRNA [NM_001002894]
AK041700;NM_026115	Mus musculus histone aminotransferase 1 (Hat1), mRNA [NM_026115]
AK046475;NM_183142	Mus musculus expressed sequence AI849156 (AI849156), mRNA [NM_183142]
NM_010094	Mus musculus left right determination factor 1 (Lefty1), mRNA [NM_010094]
NM_010068	Mus musculus DNA methyltransferase 3B (Dnmt3b), transcript variant 3, mRNA [NM_010068]
AK087334;NM_177700	Mus musculus cDNA sequence BC060631 (BC060631), mRNA [NM_177700]
NM_009989	Mus musculus cytochrome c, testis (Cyct), mRNA [NM_009989]
AK047808;NM_175138	Mus musculus dynein, axonemal, intermediate chain 1 (Dnaic1), mRNA [NM_175138]
AK035177;NM_178367	Mus musculus DEAH (Asp-Glu-Ala-His) box polypeptide 33 (Dhx33), mRNA [NM_178367]
NM_009852	Mus musculus CD6 antigen (Cd6), mRNA [NM_009852]
NM_025781	Mus musculus DNA segment, Chr 8, Brigham & Women's Genetics 1414 expressed (D8Bwg1414e), mRNA [NM_025781]
NM_173383.1;NM_173383	Mus musculus dead end homolog 1 (zebrafish) (Dnd1), mRNA [NM_173383]
AK049216;NM_172558	Mus musculus gem (nuclear organelle) associated protein 5 (Gemin5), mRNA [NM_172558]
NM_008199	Mus musculus histocompatibility 2, blastocyst (H2-BI), mRNA [NM_008199]
AK029115;NM_145993	Mus musculus l(3)mbt-like 2 (Drosophila) (L3mbtl2), mRNA [NM_145993]
AK012351;XM_125586	Mus musculus glutaminyl-tRNA synthase (glutamine-hydrolyzing)-like 1, mRNA (cDNA clone MGC:91336 IMAGE:30605375), complete cds. [BC070459]
NM_009482	Mus musculus undifferentiated embryonic cell transcription factor 1 (Utf1), mRNA [NM_009482]
NM_009337	Mus musculus T-cell lymphoma breakpoint 1 (Tcl1), mRNA [NM_009337]
AK030923;NM_173756	Mus musculus RIKEN cDNA 5830457H20 gene (5830457H20Rik), mRNA [NM_173756]
AJ007734;	Mus musculus mRNA for Z30 small nucleolar RNA. [AJ007734]
NM_025503	Mus musculus RIKEN cDNA 1700029P11 gene (1700029P11Rik), mRNA [NM_025503]

NM_133204	Mus musculus zinc finger protein 371 (Zfp371), mRNA [NM_133204]
BC026784;NM_029339	Mus musculus RIKEN cDNA 1700023O11 gene (1700023O11Rik), mRNA [NM_029339]
NM_010637	Mus musculus Kruppel-like factor 4 (gut) (Klf4), mRNA [NM_010637]
BY346895;NM_001005223	Mus musculus thyroid hormone receptor interactor 3 (Trip3), mRNA [NM_001005223]
AI848615;	
AK051027;NM_008988	Mus musculus putative neuronal cell adhesion molecule (Punc), mRNA [NM_008988]
AK014173;	Mus musculus 13 days embryo head cDNA, RIKEN full-length enriched library, clone:3110043L15 product:unknown EST, full insert sequence. [AK014173]
NM_007872	Mus musculus DNA methyltransferase 3A (Dnmt3a), transcript variant 1, mRNA [NM_007872]
BC029284;XM_489605	Mus musculus mRNA for mKIAA0128 protein [AK172894]
NM_008564	Mus musculus minichromosome maintenance deficient 2 mitotin (S. cerevisiae) (Mcm2), mRNA [NM_008564]
NM_022887	Mus musculus tuberous sclerosis 1 (Tsc1), mRNA [NM_022887]
NM_008452	Mus musculus Kruppel-like factor 2 (lung) (Klf2), mRNA [NM_008452]
AK049212;	Mus musculus ES cells cDNA, RIKEN full-length enriched library, clone:C330008D03 product:weakly similar to KRUPPEL-RELATED ZINC FINGER PROTEIN F80-L [Mus musculus], full insert sequence. [AK082760]
NM_029360	Mus musculus transmembrane 4 superfamily member 5 (Tm4sf5), mRNA [NM_029360]
NM_013584	Mus musculus leukemia inhibitory factor receptor (Lifr), mRNA [NM_013584]

Table S6. Histological Analyses of Teratomas Derived from iPS Cells

	Undiff	Ectoderm		Mesoderm			Endoderm
iPS clone		Squamous Epithelium	CNS	Bone	Cartilage	Muscle	Columnar Cell
MEF10-1	+++	+	+++	–	–	–	+
MEF10-3	+++	+	–	–	+	–	+
MEF10-6	+++	+	+++	–	+	–	++
MEF10-6 (p30)	++	+	+++	+	+	++	++
MEF10-7	++++	–	–	–	–	–	–
MEF10-10	++++	–	–	–	–	–	–
MEF4-2	++	++	+++	+	+	–	++
MEF4-7	++	++	+++	–	+	++	++
MEF4-10	++++	–	–	–	–	–	–
MEF4wt-4	++	–	+++	–	+++	++	++
MEF3-1	++++	–	–	–	–	–	–
MEF3-2	++++	–	–	–	–	–	–
MEF3-3	++++	–	–	–	–	–	–
MEF3-4	++++	–	–	–	–	–	–
MEF3-5	++++	–	–	–	–	–	–
MEF3-6	++++	–	–	–	–	–	–
TTF4-1	+	++	+++	++	++	+++	++
TTF4-3	++	+	+++	–	+	++	++
TTFgfp4-1	+	–	+++	+	++	++	++
TTFgfp4-2	+++	–	+++	–	+	–	+
TTFgfp4-3	+	+	+++	+	++	++	++

TTFgfp4-4	++	+	+++	+	++	++	++
TTFgfp4-5	+++	+	++	−	++	++	++
TTFgfp4-7	+++	++	+++	−	++	++	++
MSCgfp4-1	+++	−	+++	−	++	++	++

++++, found in >80% of tumor sections; +++, 20-80%; ++, 1-20%; +, <1%; −, not found.

Table S7. PCR-Based SSLP Analyses of iPS-MEF Clones

	MEF24-1-5	**MEF24-1-9**	**MEF24-1-18**	**MEF4-7**	**MEF10-6**	**129**	**C57/BL6**
D1Mit21	246	246	246	246	246	250	246
D4Mit15	279	279	279	279	279	329	279
D5Mit267	148	148	148	148	148	138	148
D7Mit44	170	170	170	190, 170	170	170	190
D8Mit94	156, 130	156, 130	156, 130	156, 130	156, 130	160	156, 130
D8Mit215	182	182	184	182	182	184	182
D11Mit130	201	201	201	201	201	216	201
D11Mit236	106	106	106	106	106	118	106
D12Mit99	151	151	151	151	151	173	151
D13Mit16	212	212	212	212	212	178	212
D18Mit4	121	121	121	121	121	142	121
D19Mit1	210, 170	210, 170	210, 170	170	170	170	210
DXMit64	134	134	134	134	134	114	134

Table S8. PCR-Based SSLP Analyses of iPS-TTFgfp4 Clones

	TTFgfp4-1	TTFgfp4-3	TTFgfp4-7	129	C57/BL6	ICR
D1Mit21	230	230	230	250	246	230
D4Mit15	279	279	279	329	279	279
D5Mit267	156	156	156	138	148	156
D7Mit44	198	170	170	170	190	198
D8Mit94	130	130	130	160	156, 130	130
D8Mit215	164	164	164	184	182	164
D11Mit130	210	201	201	216	201	210
D11Mit236	106, 84	106	106	118	106	84
D12Mit99	151	151	151	173	151	151
D13Mit16	212	212	212	178	212	212
D18Mit4	121, 142	121, 142	121, 142	142	121	142
D19Mit1	170	170	170	170	210	195
DXMit64	134	134	134	114	134	134

Shown are sizes of PCR products amplified from genomic DNA of iPS-TTF4 clones, RF8 ES cells (129SVJae), C57/BL6 mouse, and ICR mouse.

Table S9. Primers Used in This Study

MeOct3/4-DMR-S	GGT TTT TTA GAG GAT GGT TGA GTG	Methylation analysis of *Oct3/4*
MeOct3/4-DMR-AS	TCC AAC CCT ACT AAC CCA TCA CC	
MeNanog-F2-S	GAT TTT GTA GGT GGG ATT AAT TGT GAA TTT	Methylation analysis of *Nanog*
MeNanog-F2-AS	ACC AAA AAA ACC CAC ACT CAT ATC AAT ATA	
Fbxpro-scU488	TTT GAT TTA AAT TAT AGG TAT GAT TAA TTT	Methylation analysis of *Fbx15*
Fbxpro-scL712	ACT AAC TAA CTA ATT AAT CCA CCT TAA CAA	
Fbxpro-scU524	AGG AGA AGA TAT TAA GTA GAA ATT TTT TTT	Methylation analysis of *Fbx15* (nested)
Fbxpro-scL692	ACC TTA ACA ATT TAT CTA ACA AAC CCC TAA	
Ecat1-RT-S	TGT GGG GCC CTG AAA GGC GAG CTG AGA T	RT-PCR for *Ecat1*
Ecat1-RT-AS	ATG GGC CGC CAT ACG ACG ACG CTC AAC T	
pH34-U38	GAA GTC TGG TTC CTT GGC AGG ATG	RT-PCR for *Esg1*
pH34-L394	ACT CGA TAC ACT GGC CTA GC	
6047-S1	CAG GTG TTT GAG GGT AGC TC	RT-PCR for endogenous *Nanog*
6047-AS1	CGG TTC ATC ATG GTA CAG TC	
45328-S118	ACT GCC CCT CAT CAG ACT GCT ACT	RT-PCR for *ERas*
ERas-AS304	CAC TGC CTT GTA CTC GGG TAG CTG	
Gdf3-U253	GTT CCA ACC TGT GCC TCG CGT CTT	RT-PCR for *Gdf3*
Gdf3-L16914	AGC GAG GCA TGG AGA GAG CGG AGC AG	
Fgf4-RT-S	CGT GGT GAG CAT CTT CGG AGT GG	RT-PCR for *Fgf4*
Fgf4-RT-AS	CCT TCT TGG TCC GCC CGT TCT TA	
Oct3/4-S9	TCT TTC CAC CAG GCC CCC GGC TC	RT-PCR for endogenous *Oct3/4*
Oct3/4-AS210	TGC GGG CGG ACA TGG GGA GAT CC	
Oct3/4-U474	CTG AGG GCC AGG CAG GAG CAC GAG	RT-PCR for total *Oct3/4*
Oct3/4-L935	CTG TAG GGA GGG CTT CGG GCA CTT	

Gata6-S917	ACC TTA TGG CGT AGA AAT GCT GAG GGT G	RT-PCR for *Gata6*
Gata6-AS1250	CTG AAT ACT TGA GGT CAC TGT TCT CGG G	
T-S764	ATG CCA AAG AAA GAA ACG AC	RT-PCR for *Brachyury*
T-AS1579	AGA GGC TGT AGA ACA TGA TT	
Mtap2-S629	CAT CGC CAG CCT CGG AAC AAA CAG	RT-PCR for *Map2*
Mtap2-AS867	TGC GCA AAT GGA ACT GGA GGC AAC	
Rex1-RT-S	ACG AGT GGC AGT TTC TTC TTG GGA	RT-PCR for *Rex1*
Rex1-RT-AS	TAT GAC TCA CTT CCA GGG GGC ACT	
Utf1-RT-S	GGA TGT CCC GGT GAC TAC GTC TG	RT-PCR for *Utf1*
Utf1-RT-AS	GGC GGA TCT GGT TAT CGA AGG GT	
Cripto-S	ATG GAC GCA ACT GTG AAC ATG ATG TTC GCA	RT-PCR for *Cripto*
Cripto-AS	CTT TGA GGT CCT GGT CCA TCA CGT GAC CAT	
Dax1-S1096	TGC TGC GGT CCA GGC CAT CAA GAG	RT-PCR for *Dax1*
Dax1-AS1305	GGG CAC TGT TCA GTT CAG CGG ATC	
Zfp296-S67	CCA TTA GGG GCC ATC ATC GCT TTC	RT-PCR for *Zfp296*
Zfp296-AS350	CAC TGC TCA CTG GAG GGG GCT TGC	
Nat1-U283	ATT CTT CGT TGT CAA GCC GCC AAA GTG GAG	RT-PCR for *Nat1*
Nat1-L476	AGT TGT TTG CTG CGG AGT TGT CAT CTC GTC	
Neo-S63	GCT ATT CGG CTA TGA CTG GGC ACA	RT-PCR for *Neo*
Neo-AS581	CCA CCA TGA TAT TCG GCA AGC AGG	
Cdx2-S775	GGC GAA ACC TGT GCG AGT GGA TGC GGA A	RT-PCR for *Cdx2*
Cdx2-AS1210	GAT TGC TGT GCC GCC GCC GCT TCA GAC C	
Sox2-S768	GGT TAC CTC TTC CTC CCA CTC CAG	RT-PCR for total *Sox2*
anti-Sox2-AS	TCA CAT GTG CGA CAG GGG CAG	
Sox2-RT-S	TAG AGC TAG ACT CCG GGC GAT GA	RT-PCR for endogenous *Sox2*

Sox2-RT-AS	TTG CCT TAA ACA AGA CCA CGA AA	
mKLF4cDNAs1064	CAC CAT GGA CCC GGG CGT GGC TGC CAG AAA	RT-PCR for total *Klf4*
mKLF4cDNAas1769	TTA GGC TGT TCT TTT CCG GGG CCA CGA	
Klf4-S1236	GCG AAC TCA CAC AGG CGA GAA ACC	RT-PCR for endogenous *Klf4*
Klf4cDNAas2547	TCG CTT CCT CTT CCT CCG ACA CA	
c-Myc-S1093	CAG AGG AGG AAC GAG CTG AAG CGC	RT-PCR for total *c-Myc*
m-cMyc-AS	TTA TGC ACC AGA GTT TCG AAG CTG TTC G	
Myc-S1904	TGA CCT AAC TCG AGG AGG AGC TGG AAT C	RT-PCR for endogenous *c-Myc*
Myc-AS2042	AAG TTT GAG GCA GTT AAA ATT ATG GCT GAA GC	
6047-S4	AGG GTC TGC TAC TGA GAT GCT CTG	RT-PCR for total *Nanog*
6047-AS5	CAA CCA CTG GTT TTT CTG CCA CCG	
Nanog-exon-ChIP-S	TCT TTA GAT CAG AGG ATG CCC CCT AAG C	ChIP for *Nanog* promoter
Nanog-exon-ChIP-AS	AAG CCT CCT ACC CTA CCC ACC CCC TAT	
Oct3/4-ChIP-S1	ATC CGA GCA ACT GGT TTG TG	ChIP for *Oct3/4* promoter
Oct3/4-ChIP-AS1	CAA TCC CAC CCT CTA GCC TT	